



Centre for
Ecology & Hydrology

NATURAL ENVIRONMENT RESEARCH COUNCIL

IDMM-ag v3

An improved model for prediction of metal concentrations in soils and receiving waters of agricultural catchments

Date 16/10/2016

Title IDMM-ag v3: An improved model for prediction of metal concentrations in soils and receiving waters of agricultural catchments

Client European Copper Association, International Zinc Association

Client reference

Confidentiality, copyright and reproduction © Natural Environment Research Council, 2016.

CEH reference NEC04709

CEH contact details Stephen Lofts
NERC Centre for Ecology and Hydrology, Lancaster
Environment Centre, Lancaster LA1 4AP, U.K.

t: +44 (0) 1524 595878
f: +44 (0)1524 61536
e: stlo@ceh.ac.uk

Authors Stephen Lofts, Lee Walker

Contents

NOTE ON OCTOBER 2016 VERSION OF THE REPORT	1
1. Introduction.....	2
2. Model description	4
2.1. Summary model description	4
2.2. Detailed model description	6
2.2.1. Soil model	6
2.2.2. Surface water model	13
3. Model application	19
4. Results and Discussion	26
5. Conclusions.....	42
6. References	42
Appendices.....	45

NOTE ON OCTOBER 2016 VERSION OF THE REPORT

The previously submitted draft report (November 2015) used version 2 of the IDMM–ag. Since submission of that draft, Parts of the model dealing soil erosion have been rewritten to deal with minor errors discovered. The predictions presented in this report have been done using the updated model (IDMM–ag v3). The updated model produces results which are broadly similar to those previously obtained, both in trends across the scenarios and in the differences in surface water and sediment concentrations within different waterbody types using the same soil scenario. A single scenario (D5 pond) now has predicted PNEC exceedances for surface water copper which were not predicted by the previous model. All other patterns of PNEC exceedance or non-exceedance are the same as were predicted using the previous model.

The influence of high soil erosion rate on metal accumulation in scenario R2 was not seen when using IDMM–ag v3. Therefore, discussion of this has been removed from this version of the report.

A summary of the differences in predicted concentrations relevant to PNEC exceedance is presented in Appendix 2.

1. Introduction

Metals such as copper, zinc and lead may enter agricultural soils from a variety of different sources including atmospheric deposition, use of metal-containing substances as biocides (e.g. Bordeaux solution) or preservatives (e.g. CCA mixture for wood preservation), runoff from buildings and other structures (e.g. metal roofs and piping, galvanised power structures), and as incidental constituents of materials such as fertilisers, biosolids, manures, composts and other wastes applied to land.

Metals added to soils are typically strongly retained by the soil solids and hence repeated additions will result in buildup of metal within the soil profile. There is also increased likelihood of enrichment of local surface waters and sediments with metals over time. Although the flux of metal to surface waters may be a minor proportion of the total pool in the catchment soils, under conditions of high metal addition rates significantly elevated surface water concentrations in small agricultural catchments have been observed (Banas et al., 2010).

The high particle-reactive behaviour of metals in soils, waters and sediments means that fate and risk assessment of metal additions to soils needs to take a longer-term approach compared to assessment of other chemical such as organic pesticides, where short-term risks following application events are more important. For metals, concentrations in soils and receiving waters (including sediments) following an addition event will be highly dependent upon the history of past additions. Thus specific modelling of fate, tailored to the particular properties of metals, is needed to facilitate risk assessment.

This report presents the latest version of the Intermediate Dynamic Model for Metals (IDMM), a fate modelling framework for metals in agricultural catchments and their receiving waters. The IDMM was originally designed to simulate the dynamics of metals following atmospheric deposition to remote upland catchments of the UK (Lofts et al., 2013). The first version simulated only soil, using a single box to represent the shallow (~25–35cm depth) topsoil. Further development of the model was done under contract to EFSA in order to carry out risk assessment of the input of copper and zinc to European agricultural soils due to animal manure application (Monteiro et al., 2010). This version of the model contained multiple soil layers to simulate deeper agricultural soils. Calculation of metal concentrations in surface waters and sediments was done using the predicted fluxes of metals from soils, however no explicit surface water model was produced and risks of metals in bottom sediments were assessed on the basis of concentrations in “freshly deposited” sediment, i.e. suspended sediment. This approach, while in accordance with EU risk assessment practice (TGD, 2003), is a ‘worst case’ risk scenario which does not explicitly account for the processes controlling metal concentrations in bottom sediments. In practice, organisms are likely to be exposed to a mixture of freshly deposited and older sediments generated by deposition, resuspension and bioturbation processes.

Therefore, for more realistic fate assessment there is a need to develop the IDMM to explicitly model surface waters. The new version of the model presented here (named IDMM-ag) now includes a model of surface waters which simulates sediment and water dynamics, and the associated metal dynamics, within waterbodies. The new model is applied predictively to scenarios of copper and zinc addition to soils previously

simulated (Monteiro et al., 2010) and the contrasts between predictions in surface waters considered. Prospects for further improvement of the model are considered, particularly the potential for validation against field data.

2. Model description

2.1. Summary model description

The IDMM–ag uses a modular structure to allow catchments of varying levels of complexity to be simulated (Figure 1). A catchment contains one or more soil profiles, each representing a specific area of the catchment draining into surface water. Each profile comprises one or more soil horizons, each itself comprising one or more homogenous layers. Each layer comprises fine soil, porespace (containing air and water) and (optionally) stones. Each layer is assumed to be fully mixed.

The soil model runs on an annual timestep. Metal input to the uppermost layer of the soil horizon can move either vertically to the next layer downward, or laterally direct to surface water. Vertical movement can occur as metal dissolved in moving porewater. Lateral movement can occur either as dissolved metal or metal associated with eroded soil. Metal moving vertically out of the lowest layer in the profile is assumed to be transferred to groundwater and a component is assumed to re–emerge in baseflow to the surface waterbody. Removal of metal in crops may be simulated and if desired may be dependent upon the soil chemistry. Metal may exist in one of three main forms: labile ('geochemically active'), aged and mineral. Metal inputs may be defined as a mixture of labile and mineral forms. Metal chemistry, and the transformations among the different forms, are presented in detail in Section 0.

The surface water model runs on a daily timestep in order to consider the effect of short–term variability in flow on the time-averaged dissolved metal concentration, which represents the average exposure of biota over time. A surface water is represented by a series of one or more reaches representing either lentic (ponds) or lotic (streams, ditches). Reaches are connected linearly to form a surface water system. Each waterbody receives input fluxes of water, sediment, and associated metals from

- the reach immediately upstream, if there is one;
- lateral transfers from the soil profiles, which may represent surface runoff and/or percolation into and through field drains;
- baseflow, assumed to derive from groundwater seepage.

Each reach has a bottom sediment, comprising an upper and a lower layer. Each layer comprises a mixture of fine and coarse sediment and porewater and is modelled as being fully mixed. Sediment may enter the reach by transport from the next reach upstream (if there is one), from the soil profiles and in baseflow. Sediment may exchange between the water column and the bed (deposition and resuspension) and between the upper and lower layers (bioturbation) and be buried from the lower layer. An acid volatile sulphide (AVS) concentration may be defined for the lower layer; this sulphide may precipitate with chemically active (labile) metal rendering it nonbioavailable. Water and sediment move downstream, either to the next reach in

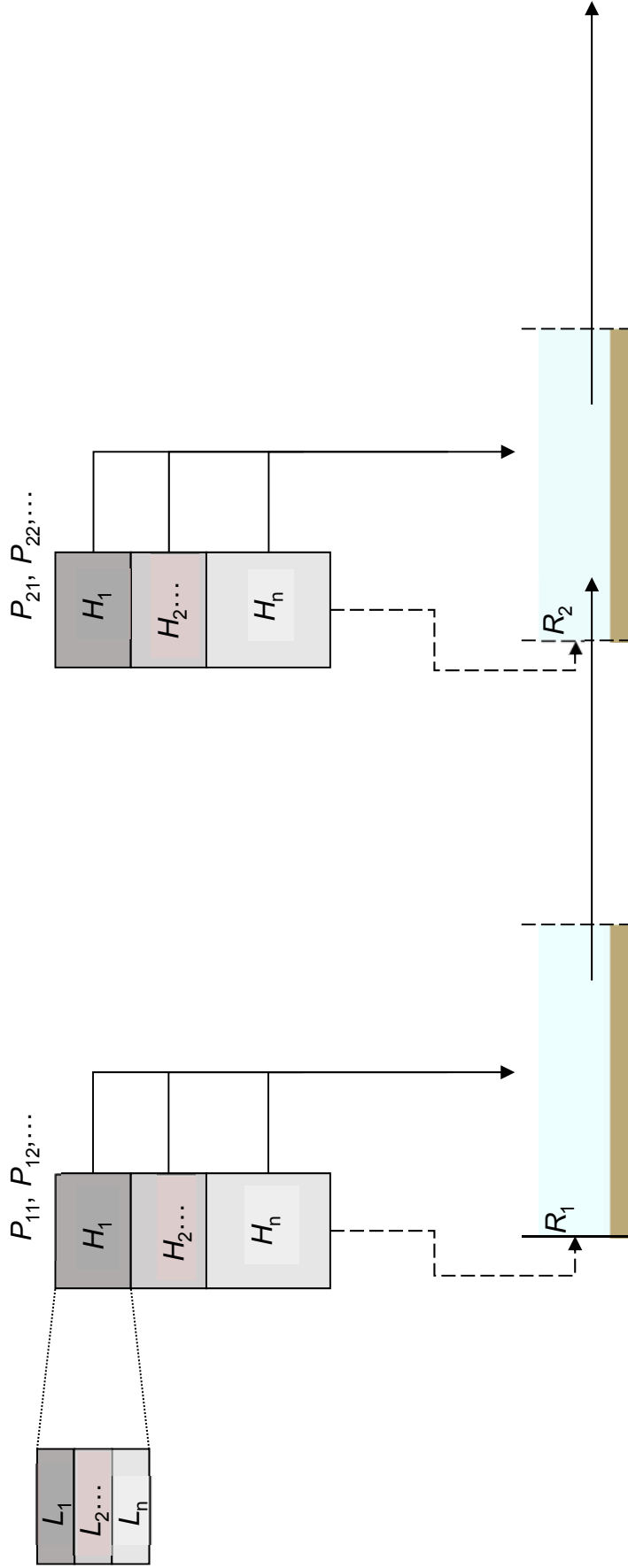


Figure 1. General schematic of IDMM-ag

sequence or out of the system. Sediment may move downstream either in the water column or as bedload.

2.2. Detailed model description

2.2.1. Soil model

Each soil profile comprises one or more soil horizons, which themselves contain one or more soil layers. A layer comprises fine soil, stones and porespace, which is partly filled with porewater, and represents a depth of soil assumed to be fully mixed. Each soil layer contains three pools of metal: labile ('geochemically active'), aged and mineral. A full explanation of these forms is given in Section 0.

Labile metal comprises dissolved metal and metal adsorbed to the surfaces of the fine soil, while aged and mineral metal are completely associated with the fine soil. On each annual timestep, a flux of metal (mol m^{-2}) enters the uppermost layer, and metal is lost from each layer vertically (to the layer below or to groundwater in the case of the lowest layer), or laterally. Lateral losses represent either losses in surface runoff or due to artificial field drainage systems. Vertical losses from the lowest layer are assumed to move to groundwater and are used in the computation of metal fluxes into the surface water in baseflow.

Metal fluxes out of each soil layer may be in dissolved form or as metal associated with eroding soil. The latter comprises adsorbed labile, aged and mineral metal. Dissolved metal fluxes are the product of the porewater concentration and the annual vertical and lateral water fluxes from the layer, i.e.

$$F_{\text{diss, vert},L} = [M]_{\text{diss},L} \cdot V_{\text{vert},L}; \quad F_{\text{diss, lat},L} = [M]_{\text{diss},L} \cdot V_{\text{lat},L}$$

where $F_{\text{diss, vert},L}$ and $F_{\text{diss, lat},L}$ are the vertical and lateral dissolved fluxes ($\text{mol m}^{-2} \text{a}^{-1}$), $[M]_{\text{diss},L}$ is the dissolved metal concentration in the porewater (mol m^{-3}) and $V_{\text{vert},L}$ and $V_{\text{lat},L}$ are the vertical and lateral water fluxes ($\text{m}^3 \text{m}^{-2} \text{a}^{-1}$). Labile adsorbed, aged and mineral metal fluxes are the product of the concentration of metal in each form and the annual vertical and lateral fluxes of eroded soil, e.g.

$$F_{\text{ads, vert},L} = \{M\}_{\text{ads},L} \cdot f_{e,L} \cdot F_{\text{ES,vert},L}; \quad F_{\text{ads, lat},L} = \{M\}_{\text{ads},L} \cdot f_{e,L} \cdot F_{\text{ES,lat},L}$$

where $F_{\text{ads, vert},L}$ and $F_{\text{ads, lat},L}$ are the vertical and lateral adsorbed labile fluxes ($\text{mol m}^{-2} \text{a}^{-1}$), $\{M\}_{\text{ads},L}$ is the labile adsorbed metal concentration in the layer ($\text{mol kg fine soil}^{-1}$) and $F_{\text{ES,vert},L}$ and $F_{\text{ES,lat},L}$ are the vertical and lateral fluxes of eroded soil ($\text{kg fine soil m}^{-2} \text{a}^{-1}$). The term $f_{e,L}$ is an optional factor for the enrichment of metals in eroded soil relative to the *in situ* (bulk) fine soil (See section *Soil erosion* for details). Corresponding expressions can be written for aged and mineral metal.

Variable, annual metal additions to the soil profile ($\text{mol m}^{-2} \text{a}^{-1}$) are defined in inputs. Additions may be delineated by source (e.g. natural deposition, anthropogenic deposition, incidental inputs in fertilisers, manures etc.). Inputs are treated as labile.

Metal speciation in soil

Computation of the speciation of metal in each soil layer is needed in order to calculate fluxes out of the layer. The three main forms of metal considered – labile, aged and mineral – represent the following species of metals:

- labile metal represents metal dissolved in the porewater and metal adsorbed to the surfaces of fine soil;
- aged metal represents metal ‘fixed’ into the fine soil solids. Metal transfer between the labile and aged forms is reversible and is modelled using first order kinetic expressions derived from laboratory studies of fixation;
- mineral metal represents metal which is strongly fixed in the soil solids, for example metal derived from the parent material during soil formation. This pool supplies metal to the labile pool through weathering, which is described by first order kinetics. This pool is replenished by kinetically-modelled transfer of metal from the aged pool.

Soil metal speciation is illustrated diagrammatically in Figure 2. The equilibrium speciation of the labile pool is done using two submodels. The concentration of adsorbed labile metal is done using empirical Freundlich–type isotherms which describe the equilibrium between the free metal ion concentration in the porewater and the adsorbed labile concentration as a function of the soil chemistry:

$$\log K_f = \log \left(\frac{\{M\}_{\text{ads}}}{[M]_{\text{free}}^n} \right) = \alpha_0 + \alpha_1 \cdot \text{pH}_{\text{pw}} + \alpha_2 \cdot \log(\% \text{OM}) + \alpha_3 \cdot \log(\% \text{clay})$$

where $[M]_{\text{free}}$ is the free metal ion concentration (mol dm^{-3}), pH_{pw} is the porewater pH, and %OM and %clay are the % organic matter and clay contents of the fine soil,

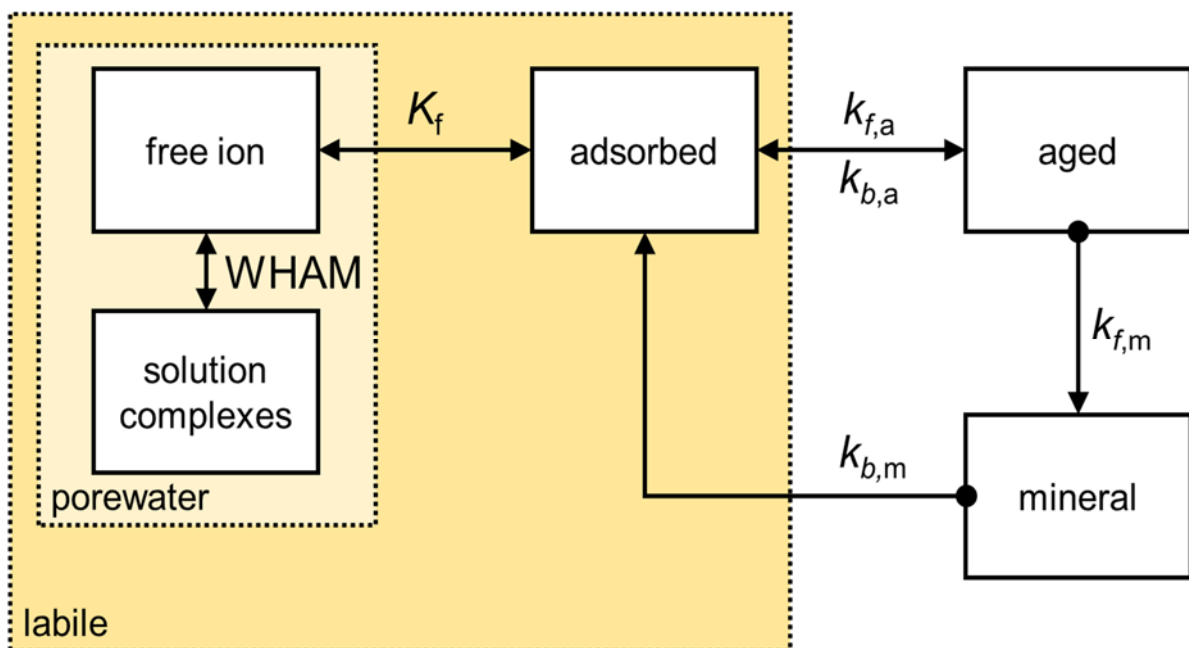


Figure 2. Schematic diagram of metal transformations in soils. Large K denotes an equilibrium transformation parameter, small k denotes a kinetic transformation parameter.

respectively. The pH_{pw} value is supplied in inputs as a driving variable, and may be varied over the time course of the simulation. The %OM and %clay values are also supplied in inputs. The %OM for the uppermost horizon may be varied over time in order to simulate temporal changes in %OM due to agricultural practices (Section *Soil organic matter changes*).

The speciation of porewater metal, i.e. the distribution between the free ion and complexed forms, is done using the mechanistic model WHAM/Model VI. This computation uses, in addition to the porewater pH, concentrations of the major ions Na, Mg, Ca, Cl, NO_3 , SO_4 , Al, Fe(III), also dissolved organic carbon (DOC), the partial pressure of carbon dioxide (pCO_2) in the soil atmosphere, and the soil temperature. Concentrations of Na, Mg, Ca, Cl, NO_3 and SO_4 are specified for each soil layer in inputs. At setup (Section *Soil profile setup*), the concentrations are adjusted to achieve electrical charge balance in the soil and the adjusted concentrations are then assumed constant throughout the simulation period. The chemistry of Al and Fe(III) in the porewater is simulated by estimation of their free ion activities as a function of pH. The free Al is estimated using the expressions derived by Tipping (2005), where the free Al activity, a_{Al} , is firstly computed as a function of pH:

$$\log a_{\text{Al}} = z_1 \cdot \text{pH}_{\text{pw}} + z_2$$

where z_1 and z_2 are constants. Different values of z_1 and z_2 are used, depending on whether the %OM content of the layer is greater than 20% or not. A parallel estimate of a_{Al} based upon solubility equilibrium with $\text{Al}(\text{OH})_3(\text{s})$ is also made:

$$\log a_{\text{Al}} = \log K_{\text{so,Al}} - 3 \cdot \text{pH}_{\text{pw}}$$

and the lower of the two activities is used in speciation calculations. This method gives a 'broken stick' profile of a_{Al} against porewater pH (Figure 3).

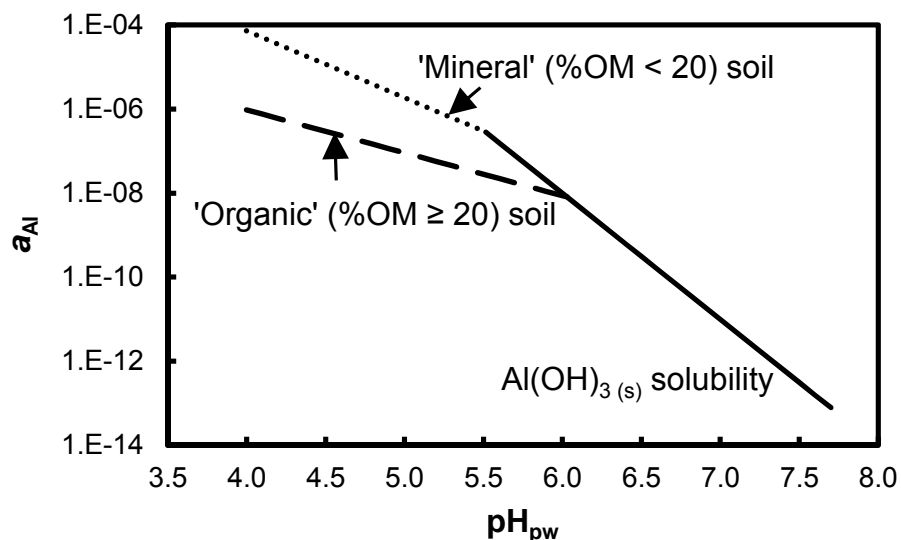


Figure 3. Profile of estimated free Al activity in soil porewater as a function of pH

The activity of Fe(III) is computed assuming it to be in equilibrium with $\text{Fe}(\text{OH})_3(\text{s})$:

$$\log a_{\text{FeIII}} = \log K_{\text{so,FeIII}} - 3 \cdot \text{pH}_{\text{pw}}$$

The soil temperature is required to adjust the equilibrium constants for solution and precipitation. An annual average, time-invariant value is specified for each layer in inputs.

Kinetically controlled transfers of metal among the labile adsorbed, aged and mineral pools are computed by first-order kinetics:

$$\frac{\Delta\{M\}_{\text{ads}}}{\Delta t} = -k_{\text{f,a}}\{M\}_{\text{ads}} + k_{\text{b,a}}\{M\}_{\text{aged}} + k_{\text{b,m}}\{M\}_{\text{min}};$$

$$\frac{\Delta\{M\}_{\text{aged}}}{\Delta t} = k_{\text{f,a}}\{M\}_{\text{ads}} - k_{\text{b,a}}\{M\}_{\text{aged}} - k_{\text{f,m}}\{M\}_{\text{aged}};$$

$$\frac{\Delta\{M\}_{\text{min}}}{\Delta t} = k_{\text{f,m}}\{M\}_{\text{aged}} - k_{\text{b,m}}\{M\}_{\text{min}};$$

where $\{M\}_{\text{aged}}$ and $\{M\}_{\text{min}}$ are the concentrations of aged and mineral metal in the soil, respectively ($\text{mol kg fine soil}^{-1}$) and $k_{\text{f,a}}$, $k_{\text{b,a}}$, $k_{\text{f,m}}$ and $k_{\text{b,m}}$ are kinetic rate constants. The timestep of computation, Δt , is one day. Therefore, metal transfers among the pools for each annual timestep are computed by repeated calculation of the daily transfers, using the above equations, for 365 iterations.

Crop metal removal

Metal may be taken up by crops removed from the soil profile. Annual removal is a function of the metal concentration in the removed crop material and the amount of material removed. The concentration of metal in the crop material is computed as a function of soil chemistry:

$$\log\{M\}_{\text{crop}} = \tau_0 + \tau_1 \cdot \text{pH}_{\text{pw}} + \tau_2 \cdot \log(\% \text{OM}) + \tau_3 \cdot \log(\% \text{clay}) + \tau_4 \cdot \log\{M\}_{\text{soil,total}}$$

where $\{M\}_{\text{soil,total}}$ is the total soil metal concentration and τ_0 to τ_4 are fixed coefficients. Because crop metal may be removed from multiple soil layers with different chemistries, the total removal is weighted:

$$F_{\text{crop}} = 0.1 \cdot Y_{\text{crop}} \cdot \sum_1^I \{M\}_{\text{crop},I} \cdot c_I$$

where F_{crop} is the annual metal removal flux (mol m^{-2}), Y_{crop} is the annual crop yield ($\text{tons dry matter ha}^{-1}$) and 0.1 is a unit conversion factor. The term $\{M\}_{\text{crop},I}$ is effectively the crop metal concentration that would be computed if all layers from which metal may enter the crop had the chemistry of layer I ($\text{mol kg dry matter}^{-1}$), and the term c_I is a layer specific 'crop factor' that adjusts the computed metal removal flux. The 'crop factor' in effect accounts for the varying uptake of metal by the crop with depth in the soil (due to variations in root mass and density) and the sum of these factors for each soil profile should be set to unity. Deep soil layers for which no crop uptake is assumed have their c_I value set to zero.

Soil management

The IDMM–ag allows tillage of the uppermost horizon to be simulated. A starting year for tillage may be specified. Tillage is simulated by mixing the fine soil, water and associated metals evenly through the horizon. Where tillage is to be simulated, the depth of the uppermost horizon should be set equal to the tillage depth.

Soil organic matter changes

Agricultural practices may change the amount of soil organic matter (OM) within the upper soil over time. For example, many temperate regions have seen long–term declines in OM over time (Gregory et al., 2015) although inputs of materials such as manures have been shown to increase topsoil OM over time (Zhang et al., 2013). The IDMM–ag allows changes in topsoil OM to be simulated by specifying a target OM for each year of simulation.

Soil hydrology

Each layer in the profile has an associated annual percolation (vertical drainage) and leaching (lateral drainage) volume specified in inputs. Percolation and leaching volumes are specified annually, so the effects of variations over time may be simulated. Each layer must have an annual percolation volume greater than zero, while annual leaching volumes may be set to zero. Leaching is intended to simulate either runoff from the uppermost (surface) layer or leaching to field drains at depth. Leaching water is routed directly to the surface water.

Soil erosion

Erosion of soil to surface waters may be a significant transport process for metal transfer to surface waters. The IDMM–ag simulates erosion by allowing soil and associated OM and metals to be removed from each layer annually in leaching. Removed (eroded) soil is routed directly to surface water. Fluxes of erosion are specified annually so that temporal changes in erosion fluxes may be simulated. Eroded soil may also be removed from the lowest layer in percolation to groundwater. This eroded soil is not routed directly to surface water, but the concentration of eroded soil in baseflow entering the surface water is set equal to the concentration in the bottom layer percolation.

Erosion may be simulated on a strict mass balance basis (where eroded soil is considered lost from the layer) or on a simpler basis where eroded soil is assumed to be replaced by the same mass of soil with the same organic matter content (thus automatically preserving the set depth of the eroding layer). In most scenarios the latter simulation method is likely to provide a sufficient approximation; however in highly eroding systems (likely to be scenarios with considerable surface runoff) this is less satisfactory. Therefore the model allows erosion to be simulated on a mass balance basis, by allowing replenishment of the soil profile. On each timestep, after erosion and soil loss have been computed, the model readjusts the boundaries between layers in order to preserve the set layer depths. This is done by moving soil and associated metal up from the layer below until the original layer depth is re–established. To preserve the set layer depths for the entire profile, this computation must be done for all layers, starting with the uppermost. The set depth of the lowest layer, and thus of

the entire profile, is preserved by replenishing the lowest layer with soil of the same physicochemical properties and metal content.

A particular feature of soil erosion with respect to the transfer of metals (and indeed other chemicals) is the observed enrichment of eroded soil with these chemicals relative to the bulk (source) soil (e.g. Quinton and Catt, 2007 for metals). This may be considered in the IDMM–ag by specifying an enrichment factor for the metal content of eroded soil relative to bulk soil.

Soil profile setup

The soil submodel, and indeed the IDMM–ag overall, simulates scenarios from an initial time in the past assumed to represent ‘pristine’ conditions. In the scenarios presented here this time was set to the year 1745 and assumed to represent a point prior to land clearance for agriculture, with metal inputs due only to natural (geogenic) deposition from the atmosphere.

Soil model initialisation entails finding the steady state labile, aged and mineral pools of metal in each layer of each profile. The steady state pools are those which do not change over time under conditions of constant metal input, i.e. where the fluxes of each form of metal into and out of each layer are balanced. For metals, the steady state flux out of each layer is given by:

$$F_{\text{diss,SS}} = ([M]_{\text{diss,SS}} + \{M\}_{\text{ads,SS}} \cdot [ES]_{\text{SS}} \cdot f_e) \cdot (V_{\text{vert,SS}} + V_{\text{lat,SS}});$$

$$F_{\text{aged,SS}} = \{M\}_{\text{aged,SS}} \cdot [ES]_{\text{SS}} \cdot f_e \cdot (V_{\text{vert,SS}} + V_{\text{lat,SS}});$$

$$F_{\text{min,SS}} = \{M\}_{\text{min,SS}} \cdot [ES]_{\text{SS}} \cdot (V_{\text{vert,SS}} + V_{\text{lat,SS}});$$

$$F_{\text{tot,SS}} = F_{\text{diss,SS}} + F_{\text{aged,SS}} + F_{\text{min,SS}} = F_{\text{input,SS}};$$

where $[ES]_{\text{SS}}$ is the eroded soil concentration (kg dm^{-3}) and f_e is the factor giving the enrichment of eroded soil in metals. Steady state relationships among the labile, aged and mineral pools must also be established. This is done by assuming that the rates of transformation among the pools are zero.

$$\frac{\Delta\{M\}_{\text{ads}}}{\Delta t} = -k_{f,a} \{M\}_{\text{ads}} + k_{b,a} \{M\}_{\text{aged}} + k_{b,m} \{M\}_{\text{min}} = 0;$$

$$\frac{\Delta\{M\}_{\text{aged}}}{\Delta t} = k_{f,a} \{M\}_{\text{ads}} - k_{b,a} \{M\}_{\text{aged}} - k_{f,m} \{M\}_{\text{aged}} = 0;$$

$$\frac{\Delta\{M\}_{\text{min}}}{\Delta t} = k_{f,m} \{M\}_{\text{aged}} - k_{b,m} \{M\}_{\text{min}} = 0.$$

The mineral pool may be set up in one of two ways. Values of $k_{f,m}$ and $k_{b,m}$ may be specified and the pool size at steady state thus computed. Alternatively, the steady state mineral pool may be specified and $k_{b,m}$ computed. This allows the total metal pool at steady state to be fixed *a priori*.

The initial setup involves adjusting the major ion composition of the porewater to electrical neutrality. This is done by an initial calculation to establish whether cations

or anions are in excess, followed by adjustment of NO_3 and SO_4 , or Mg and Ca, respectively, to achieve charge balance. The initial setup also checks for oversaturation with respect to calcite, $\text{CaCO}_3(\text{s})$. If oversaturation with calcite may be predicted either on the initial calculation or if the Mg and Ca concentrations are being adjusted to correct for an excess of negative charge. If oversaturation is predicted then the calculation mode is switched to fix the Ca free ion activity,

$$a_{\text{Ca}^{2+}} = \frac{K_{\text{sp, CaCO}_3}}{a_{\text{CO}_3^{2-}}} = \frac{K_{\text{sp}} \cdot a_{\text{H}^+}^2}{p\text{CO}_2 \cdot K_{\text{CO}_2}},$$

the major ion concentrations are fixed and the charge balanced by adjusting pH_{pw} .

After charge balancing, the steady state metal pools are then found by an iterative computation:

- 1) The free metal ion activity is estimated and the dissolved and adsorbed concentrations at equilibrium computed;
- 2) The steady state aged concentration is computed:

$$\frac{\Delta\{M\}_{\text{aged}}}{\Delta t} = k_{\text{f,a}}\{M\}_{\text{ads}} - k_{\text{b,a}}\{M\}_{\text{aged}} - k_{\text{f,m}}\{M\}_{\text{aged}} = 0, \text{ so}$$

$$\{M\}_{\text{aged}} = \{M\}_{\text{ads}} \cdot \frac{k_{\text{f,a}}}{k_{\text{b,a}} + k_{\text{f,m}}}$$

- 3) The mineral pool is either found:

$$\frac{\Delta\{M\}_{\text{min}}}{\Delta t} = k_{\text{f,m}}\{M\}_{\text{aged}} - k_{\text{b,m}}\{M\}_{\text{min}} = 0, \text{ so}$$

$$\{M\}_{\text{min}} = \{M\}_{\text{aged}} \cdot \frac{k_{\text{f,m}}}{k_{\text{b,m}}};$$

or the value of $k_{\text{b,m}}$:

$$k_{\text{b,m}} = \frac{\{M\}_{\text{aged}}}{\{M\}_{\text{min}}} \cdot k_{\text{f,m}}$$

- 4) The total flux of metal from the layer is calculated and compared with the input flux. If they agree to within defined precision limits then the steady state is considered to have been found. If not, then the estimated free metal ion activity is adjusted and the computation repeated.

For the uppermost layer, the input flux is that coming from natural atmospheric deposition. For the lower layer, the input flux is that in percolation from the layer above:

$$F_{\text{input,SS}} = ([M]_{\text{diss,SS}} + \{M\}_{\text{ads,SS}} \cdot [\text{ES}]_{\text{SS}} \cdot f_e + \{M\}_{\text{aged,SS}} \cdot [\text{ES}]_{\text{SS}} \cdot f_e + \{M\}_{\text{min,SS}} \cdot [\text{ES}]_{\text{SS}}) \cdot V_{\text{vert,SS}};$$

The steady state is computed for each layer starting from the uppermost, in order to be able to calculate the steady state input flux to the layer below.

A flexible approach to considering inputs of water, fine sediment (i.e. eroded soil) and metals to the surface water reaches is taken in the IDMM–ag. Each reach is considered to receive inputs from a defined area (m²) of subcatchment. The soil within this subcatchment is defined by one or more soil profiles, each making up a defined proportion of the subcatchment area.

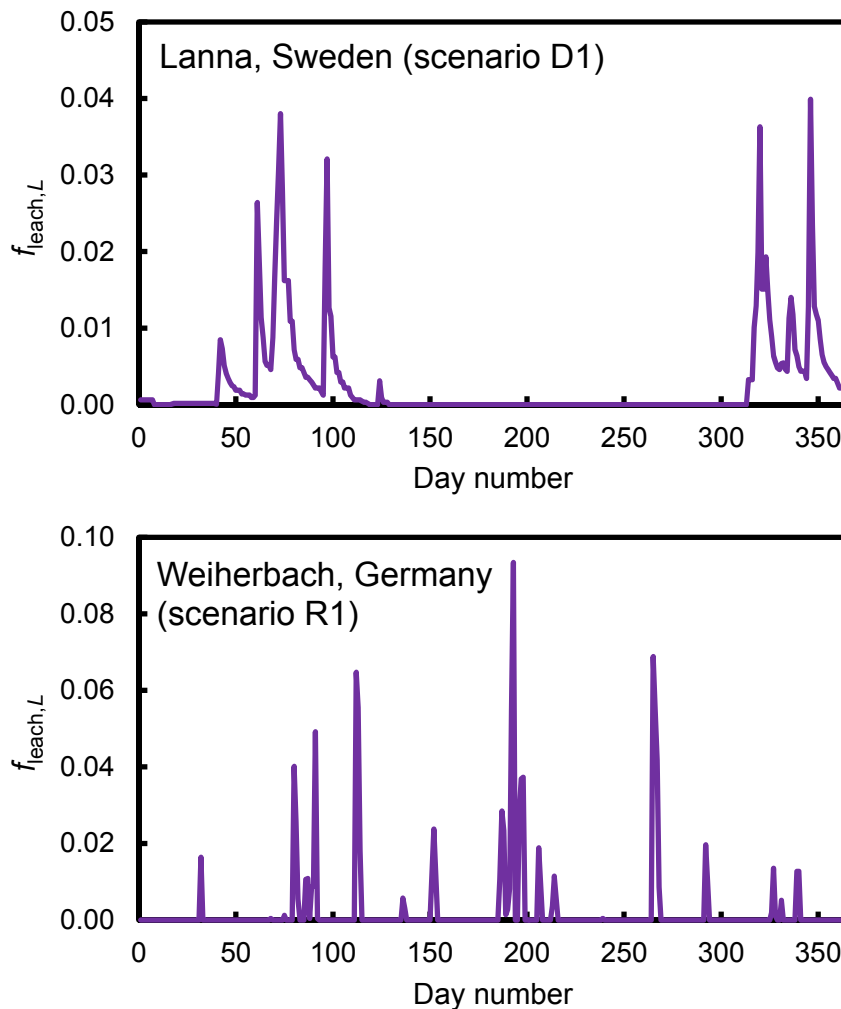


Figure 5. Example pattern of daily $f_{\text{leach},L}$ values for two of the scenarios modelled.

The surface water model runs on a timestep of no more than one day in order to capture short-term temporal variability in soilflow inputs. This variability in soilflow creates short-term variability in surface water metal concentrations, which has important implications for prediction of organism exposure over time. Since the fluxes of water, eroded soil and metals from the soil profile(s) are computed annually, they must be disaggregated to estimate daily fluxes into surface water. This is done by specifying, for each soil layer in each profile, a daily pattern of fluxes consisting of 365 values representing the proportions of the annual fluxes of water, eroded soil and metals transferred to surface waters. The proportion values are termed $f_{\text{leach,daily},L}$. Figure 5 shows an example of such a soilflow pattern. Daily fluxes of water are computed using the expression

$$V_{\text{lat},L,\text{daily}} = V_{\text{lat},L} \cdot f_{\text{leach},\text{daily},L}$$

Metal fluxes are computed using

$$F_{\text{diss, lat, } L,\text{daily}} = F_{\text{diss, lat, } L} \cdot f_{\text{leach},\text{daily},L} = [\text{M}]_{\text{diss, } L} \cdot V_{\text{lat, } L} \cdot f_{\text{leach},\text{daily},L}$$

using dissolved metal as an example. Parallel expressions can be written for the other metal forms and for eroded soil.

For a whole soil horizon we can write

$$F_{\text{diss, lat, } H,\text{daily}} = \sum_1^L F_{\text{diss, lat, } L,\text{daily}} = \sum_1^L [\text{M}]_{\text{diss, } L} \cdot V_{\text{lat, } L} \cdot f_{\text{leach},\text{daily},L}$$

and for a whole profile

$$F_{\text{diss, lat, } P,\text{daily}} = \sum_1^H F_{\text{diss, lat, } H,\text{daily}} = \sum_1^H \sum_1^L F_{\text{diss, lat, } L,\text{daily}} = \sum_1^H \sum_1^L [\text{M}]_{\text{diss, } L} \cdot V_{\text{lat, } L} \cdot f_{\text{leach},\text{daily},L}$$

To calculate the daily metal flux in soilflow into the reach ($F_{\text{diss,soilflow},R,\text{daily}}$; mol m⁻²) into each reach it is necessary to define the (sub)catchment area represented by each soil profile, A_P (m²) and the proportion of the soilflow into the reach coming from each profile, $f_{\text{SW},P}$:

$$F_{\text{diss,soilflow},R,\text{daily}} = \frac{\sum_1^P A_P \cdot f_{\text{SW},P} \cdot F_{\text{diss, lat, } P,\text{daily}}}{\sum_1^P A_P \cdot f_{\text{SW},P}}$$

Annual catchment baseflow to surface water, V_{base} (m³ m⁻² a⁻¹) is specified in inputs and assumed to be divided equally among all the profiles contributing to inflows to each reach. Baseflow supplies water, fine sediment and metals to the reach, as does soilflow. Baseflow is assumed to be constant and so daily baseflow, $V_{\text{base,daily}}$, is V_{base} divided by 365. Concentrations of fine sediment and metals in baseflow from each subcatchment are fixed to equal the area-weighted average of the concentrations in percolation out of the bottom of each contributing soil layer. So, for example, the daily flux of dissolved metal from baseflow into the reach ($F_{\text{diss,baseflow},R,\text{daily}}$; mol m⁻²) is given by the expression

$$F_{\text{diss,baseflow},R,\text{daily}} = \frac{\sum_1^P A_P \cdot f_{\text{SW},P} \cdot F_{\text{diss,vert},P,\text{daily}} \cdot \frac{V_{\text{base}}}{V_{\text{vert},P} \cdot f_{\text{leach},\text{daily},P} \cdot 365}}{\sum_1^P A_P \cdot f_{\text{SW},P}}$$

where $V_{\text{vert},P}$ is the annual water flux from the base of a soil profile and $f_{\text{leach},\text{daily},P}$ is the daily proportion of the annual flux of water percolating from the base of the soil profile. Parallel expressions can be written for the fluxes of the other metal forms and for eroded soil in baseflow.

Instream computations

Each reach is modelled as a completely mixed reactor using a variable length timestep of up to a day. The volume of water in the reach is kept constant and the daily volume of water entering the reach is subdivided, if necessary, into a set of subdaily inflow volumes smaller than the reach volume. So for example if the inflow volume for a particular day is between nine and 10 times the reach volume, the daily inflow is subdivided into 10 inflows each of 1/10th the total, and the routing for the day is simulated over ten timesteps.

The sequence of calculations for each timestep is as follows. Firstly a volume equal to the inflow is removed and inflow mixed with the remaining water. Inputs and removal of sediment from the reach. Settling of fine sediment is simulated using a sedimentation velocity specified in inputs:

$$F_{S, \text{settling}} = \frac{U_{\text{settling}}}{s \cdot D_{\text{sw}}} \cdot S_{\text{reach}}$$

where $F_{S, \text{settling}}$ is the mass of settling sediment (kg), U_{settling} is the sedimentation velocity (m/d), s is the number of timesteps for the simulation day, D_{sw} is the depth of the waterbody (m) and S_{reach} is the mass of suspended sediment in the reach following mixing in of the inflow (kg). If the ratio of settling sediment to total sediment exceeds 0.9 then it is fixed to this value, to prevent complete loss of sediment from the water column.

Fine sediment resuspension is computed using the expression

$$F_{S, \text{resusp}} = \frac{A(Q - Q_{\text{thr}})^\mu}{s} \text{ if } Q > Q_{\text{thr}}; F_{S, \text{resusp}} = 0 \text{ if } Q \leq Q_{\text{thr}},$$

where $F_{S, \text{resusp}}$ is the mass of fine sediment resuspending in the timestep (kg) and Q is the discharge through the reach (m³/s). The term Q_{thr} is a fixed threshold discharge below which resuspension does not occur, and the terms A and μ are fixed parameters. The flow rate Q is computed as

$$Q = \frac{V_{\text{in,daily}}}{86400}$$

where $V_{\text{in,daily}}$ is the daily inflow volume (m³/d).

Bottom sediment loss via downstream bedload transport is computed using the expression

$$F_{S, \text{dstr,bedload}} = \frac{m \cdot (S_{\text{upper}} + S_{\text{lower}})}{L_{\text{sw}} \cdot s}$$

where $F_{S, \text{dstr,bedload}}$ is the downstream flux in bedload (kg), S_{upper} and S_{lower} are the masses of fine sediment in the upper and lower layers respectively (kg), and m is a

bedload transport rate constant (m/d) defined in inputs. If there is an upstream reach then there will be a corresponding input of fine sediment to the upper layer via bedload transport.

Following computation of bottom sediment gains and losses, the sediment layers are mixed to simulate bioturbation effects. Bioturbation–driven mixing is simulated by defining a mass of fine sediment, S_{mix} (kg) the mass of fine sediment in the upper layer which exchanges with a similar mass of fine sediment from the lower layer:

$$S_{\text{mix}} = \frac{k_{\text{bio}} \cdot s}{(|S_{\text{lower}} - S_{\text{upper}}|) \cdot 86400}$$

where k_{bio} is a bioturbation rate constant, defined in inputs. The new depths of the two sediment layers are then computed, based on the amounts and densities of the sediment constituents and fixing the boundary between the layers such that the upper layer depth is its fixed value. If the lower layer depth exceeds its fixed value, fine sediment is buried to make the depth equal to the fixed depth. Finally WHAM/Model VI is used to compute equilibrium speciation in the lower sediment layer (including metal precipitate formation with AVS), and in the water column (including labile adsorbed pools). In these calculations the organic matter content of the fine sediment is key variable. It can be fixed to a constant value in inputs, or be determined by the organic matter content of the incoming fine sediment. The chemistry of the water column and sediment layers (pH and DOC, Na, Mg, Al, K, Ca, Fe(III), Cl, NO₃, SO₄ concentrations and $p\text{CO}_2$) is specified in inputs, with the exception of Al and Fe(III) for which the free ion activities are computed assuming equilibrium with their hydroxides.

Water column and sediment chemistry

On each timestep, resuspended sediment resuspended into the water column, and associated metal, is mixed with sediment in the water column and the distribution of metal between the dissolved and labile adsorbed forms computed using a partition coefficient approach:

$$[M]_{\text{diss}} = \frac{[M]_{\text{diss+ads}}}{1 + K_d \cdot [SS]}$$

where $[M]_{\text{diss+ads}}$ is the sum of the dissolved and labile adsorbed metal (mol dm⁻³), $[M]_{\text{diss}}$ is the dissolved metal concentration in equilibrium with the labile adsorbed pool, $[SS]$ is the suspended sediment concentration (kg dm⁻³) and K_d is the partition coefficient (dm³ kg⁻¹). The K_d is computed using WHAM/Model VI on the first timestep of each year, then stored and used for the remainder of the year.

Metal speciation using WHAM/Model VI is also done for the lower sediment in order to compute the amounts of metals bound to AVS. Sediment porewater chemistry, comprising pH and concentrations of DOC and major ions, is specified for each reach. Speciation computations are done on the sum of the labile (adsorbed) and AVS–bound pools. Metal entering from the upper sediment in labile form is added to this pool.

No computations are done on the aged or mineral pools.

Surface water setup

As with each soil layer, the 'pristine' steady state of the surface water must be established. This means that the annual time-averaged dissolved metal concentrations and the year-end concentrations of metals in sediments must be constant. In practice it is sufficient to ensure that the sediment concentrations are constant as steady state for the dissolved concentrations is always reached more rapidly than for the sediment concentrations. Steady state is found by iteratively running the model with 'pristine' inputs of water, metals and eroded soil in soilflow and baseflow, until steady metal concentrations in both sediment layers are achieved within defined precision limits (0.01% error in concentrations from one year to the next).

3. Model application

The model has been applied to the FOCUS surface water scenarios (FOCUS, 2001), previously used for risk assessment of copper and zinc additions to soil in animal manures (Monteiro et al, 2010). Basic characteristics of the scenarios are given in Table 1.

Table 1. Basic characteristics of the FOCUS scenarios. Bracketed topsoil pH_{ss} values were adjusted to 7.6 on setup on assumption of porewater equilibrium with calcite.

Scenario code	Scenario location	Surface waters	Topsoil texture	Topsoil pH _{ss}	TOPSOIL %OM	TOPSOIL %CLAY
D1	Lanna, Sweden	ditch stream	Silty clay	(7.7) ^a	4.0	47
D2	Brimstone, UK	ditch stream	Clay	(7.7) ^a	4.8	55
D3	Vredepeel, Netherlands	ditch	Sand	6.0	4.6	3
D4	Skousbo, Denmark	pond stream	Loam	7.4	2.6	12
D5	La Jaillerie, France	pond stream	Loam	7.1	3.8	20
D6	Vayia Thiva, Greece	ditch	Clay loam	(7.9) ^a	2.4	30
R1	Weierbach, Germany	pond stream	Silt loam	(7.8) ^a	2.4	13
R2	Valadares, Portugal	stream	Sandy loam	5.4	6.8	13
R3	Ozzabi, Italy	stream	Clay loam	(8.3) ^a	2.0	34
R4	Roujan, France	stream	Sandy clay loam	(8.7) ^a	1.2	25

^a adjusted to 7.6 to account for calcite solubility effect on setup.

Scenario setup

The FOCUS scenarios represent small agricultural catchments and comprise an area of soil draining into a specified surface water. The surface water types are given in Table 1. The soil was simulated by a single profile, i.e. it was assumed to be physicochemically homogeneous. Catchment areas and surface water dimensions are described in the section *Surface water setup*.

Simulations were run from 1745 to 2060. Agricultural activity was assumed to begin in 1750. For the steady state setup and the years 1745–1749 the soil profile hydrology and erosion differed from the post–1750 agricultural period. Details are given in the section *Hydrology and erosion*.

Soil structure

The FOCUS scenarios are subdivided into two categories: those for which soil–water fluxes are dominated by field drainage (D scenarios) and those for which they are

dominated by surface runoff (R scenarios). In both cases a common structure of soil horizons and layers was used:

- A top horizon (H1) comprising two layers, L1 (5cm deep) and L2 (10cm deep). This horizon represents the tilled depth of soil. Soilflow is assumed to be generated in L1 and to transfer to surface water either in bypass flow to drains or in surface runoff.
- A middle horizon (H2) comprising a single layer 15cm deep. H1 and H2 together (0–30cm depth) comprise the part of the horizon for which soil metal concentrations are reported.
- A lower horizon (H3) comprising a single layer extending from 30cm depth either to drain depth or to the base of the soil profile.

Soil chemistry

Parameters for computing the equilibrium distribution of copper and zinc between the free ion and adsorbed labile form were taken from Groenenberg et al. (2010).

Parameters for the aging of copper and zinc were partly derived from the studies of Ma et al. (2006) and Crout et al. (2006) respectively. These studies looked at the temporal declines in the labile metal pool across a range of soils spiked with metal salts, over 360 days and 813 days respectively. The data were used to derive values of the rate constants $k_{f,a}$ and $k_{b,a}$, i.e. the transformations between the labile and aged pools, assuming that transfers to and from the mineral pool were negligible on the experimental timescales. Pairs of pH_{ss} -dependent rate constants were derived to account for the clear effect of pH_{ss} on the aging rates. For copper the rate constants were given by

$$\log k_{f,a} = -2.5 + 10^{-3.3} e^{\text{pH}_{\text{ss}}} \text{ and } \log k_{b,a} = -2.1 + 10^{-3.5} e^{\text{pH}_{\text{ss}}},$$

and for zinc

$$\log k_{f,a} = -4.2 + 0.26 \cdot \text{pH}_{\text{ss}} \text{ and } \log k_{b,a} = -3.2.$$

Example predictions of the parameterised aging models are shown in Figure 6, showing the pH_{ss} effect on the degree of aging.

Long-term aging was setup by (i) setting the rate constants for metal transfer from the aged to the mineral pool ($k_{f,m}$) to 10^{-5} for both metals, and (ii) Calculating the rate constants for metal weathering from the mineral to the labile pool ($k_{b,m}$) by fixing the 'pristine' total metal concentration in each soil layer. Separate 'pristine' total metal concentrations were set for the 0-30cm soil and the sub-30cm soil, by iteratively running the model, adjusting the 'pristine' totals until the predicted present day totals agreed with values estimated from the FOREGS database (Salminen et al., 2005) by distance-weighted interpolation using the five FOREGS sampling locations nearest to each scenario.

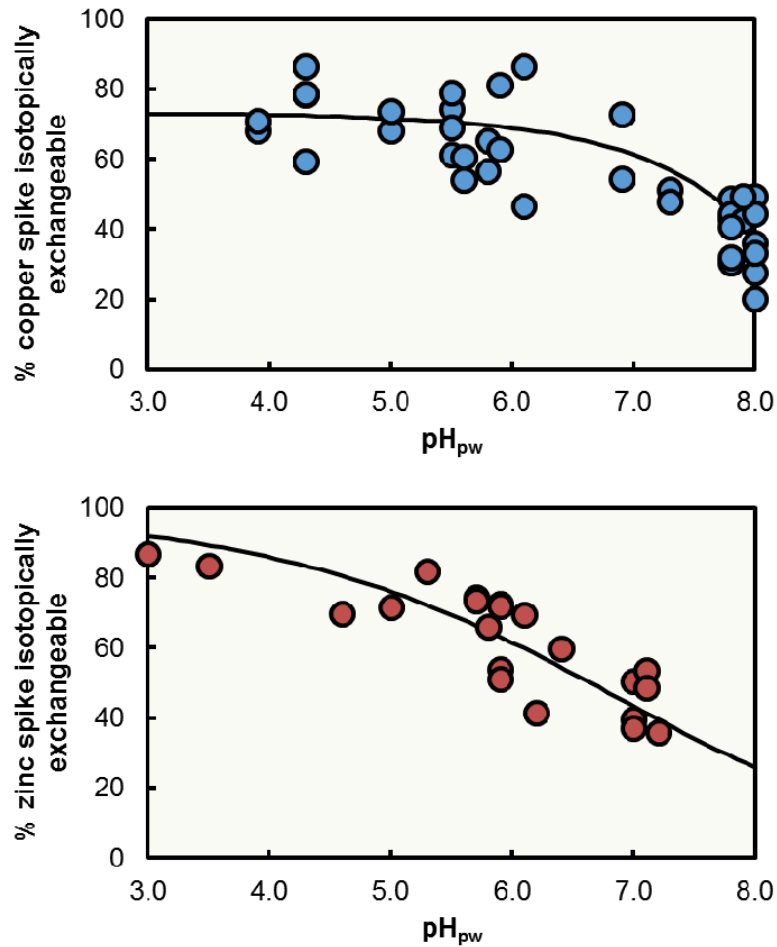


Figure 6. Predictions of the parameterised aging models for copper (top) and zinc (bottom). Points: observed lability of spiked metals in soils as a function of pH after 360 days of incubation (copper; Ma et al., 2006) and 291 days of incubation (zinc; Crout et al., 2006). Lines are the predictions of the parameterised aging models.

Concentrations of DOC in the soil porewaters are important in controlling metal fluxes through and out of the soil profiles. Concentrations were set to 15 mg dm^{-3} in Horizon 1, 10 mg dm^{-3} in Horizon 2 and 3 mg dm^{-3} in Horizon 3.

The enrichment factor, f_e was set to three for the uppermost soil layer (0–5cm), which is the source of eroded soil and metals in soilflow to surface water. For the other layers no enrichment factor was applied. We also repeated simulations with the factor set to unity to investigate its importance.

Manure was assumed to have been applied to the catchment from 1750 onwards and to have increased the soil organic matter content in Horizon 1. A model for the increase in % soil organic matter content, imposing a non-linear increase in %SOM of four up to 2060, was used to generate a change in %SOM over time. An example, for scenario D1, is given in Figure 7.

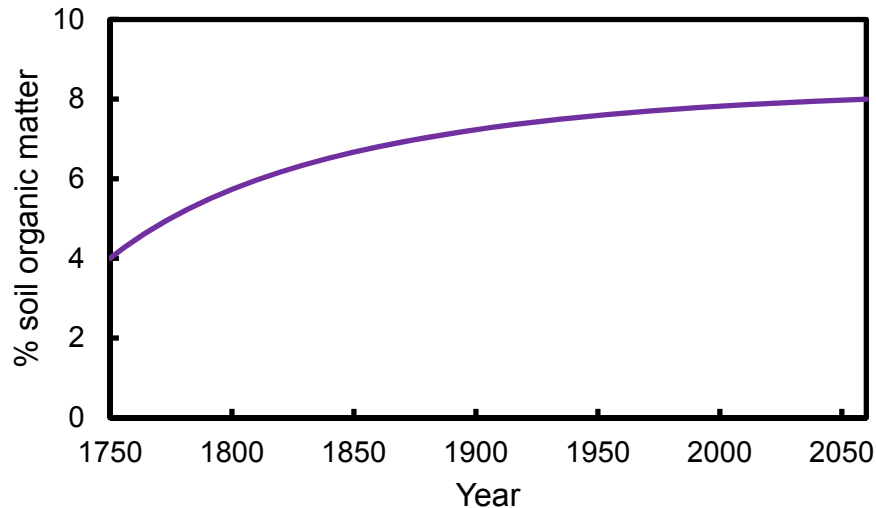


Figure 7. Example of change in % soil organic matter in Horizon 1, for scenario D1.

Metal inputs

Four sources of metal to the catchment soils were simulated: geogenic atmospheric deposition, anthropogenic atmospheric deposition, fertiliser application and manure application. Geogenic deposition was estimated using the data of Nriagu (1996), and inputs due to anthropogenic deposition, fertiliser application and manure application were estimated following the approach taken by Monteiro et al. (2010). Anthropogenic

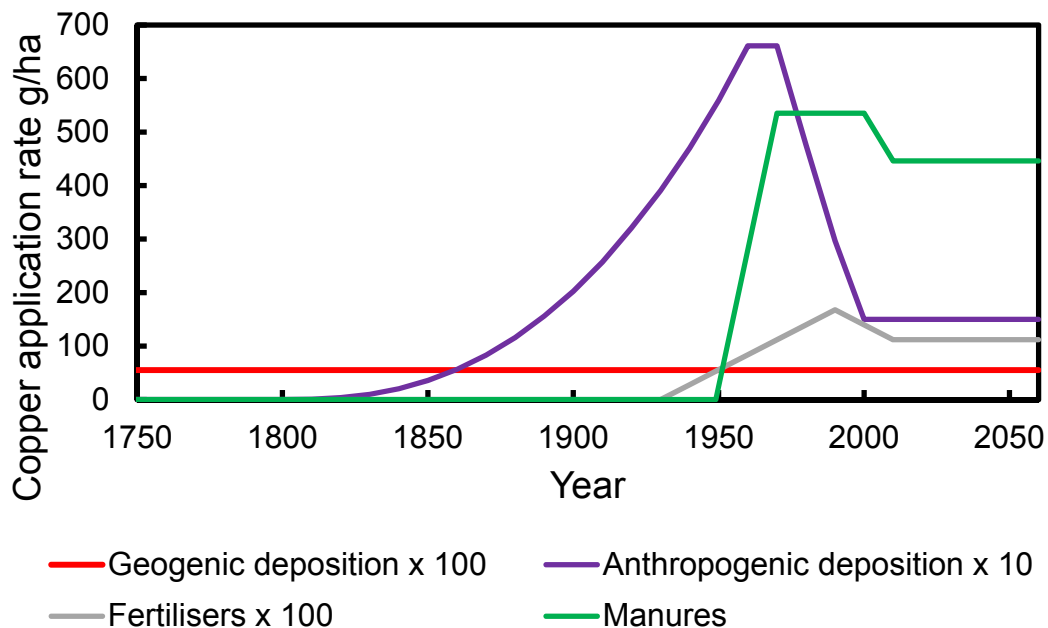


Figure 8. Example deposition trends for copper in scenario D1, assuming the manure source to be fattening pigs.

deposition and fertiliser use are assumed to result in scenario-specific inputs. Inputs due to manure vary according to the livestock type after Monteiro et al. (2010). A set of example deposition trends for copper is shown in Figure 8. The same temporal trends in inputs are assumed for zinc. All the inputs were assumed to be 100% in labile form. For this report, in order to focus comparisons with previous work, we have simulated one type of manure input and the corresponding metal inputs: that for the manure of fattening pigs, with input rates assuming that the soil is nitrogen vulnerable, i.e. that there is a maximum allowable N input rate of 170 kg ha⁻¹ a⁻¹. The characteristic input rates for this manure type are 446 g Cu ha⁻¹ a⁻¹ and 2678 g Zn ha⁻¹ a⁻¹, which were calculated using the method of Scientific Committee for Animal Nutrition (SCAN) (EC, 2003a; EC, 2003b). Inputs are assumed to begin in 1950 and rise linearly to 120% of the characteristic rate in 1970, remain constant to 2000 and decline linearly to the characteristic rate in 2010 after which they are maintained constant. For comparison, the ranges of characteristic input rates previously simulated, to represent a range of manure types, are 239–2365 g Cu ha⁻¹ a⁻¹ and 1675–3815 g Zn ha⁻¹ a⁻¹ on nitrogen-vulnerable soils, and 492–4868 g Cu ha⁻¹ a⁻¹ and 3448–6556 g Zn ha⁻¹ a⁻¹ on nitrogen-nonvulnerable soils.

Hydrology and erosion

For the D scenarios, soil hydrology (annual volumes of drainage at 5cm, 15cm and 30cm, percolation below field drain depth, and to field drains) were computed using the MACRO model (Larsbo and Jarvis, 2003) using the parameters provided by FOCUS (FOCUS, 2001). Annual volumes of water were computed by averaging the model predictions based on the multi-year meteorological, soil and crop parameters provided in FOCUS. For the period 1750 to 2060 the water predicted to pass to field drains was assumed to derive from the 0–5cm layer, i.e. the drainflow was assumed to have entered the drains in bypass flow originating in the topsoil. This is a worst case scenario for metal transfers to surface water since it assumes that drainage developed in the 0–5cm layer during rain events passes directly to drains rather than being intercepted by the soil profile. For setup and the pre-agricultural period 1745–1749 this water was assumed to pass into the layer below (5–15cm). The annual pattern in drainage from the 0–5cm layer was obtained from MACRO outputs, from the daily volumes of water flow to field drains for a one year simulation period.

MACRO does not simulate soil erosion. Ulén (1995) estimated sediment losses to drainage in the range 111–472 kg ha⁻¹ a⁻¹ for the Lanna site in Sweden (the location of scenario D1), a soil with a clay content of ~50%. This gives a midpoint value of 292 kg ha⁻¹ a⁻¹ (0.03 kg m⁻² a⁻¹). Petersen et al. (2004) measured annual sediment fluxes of between 0.92 and 4.3 kg ha⁻¹ a⁻¹ (0.000092–0.00043 kg m⁻² a⁻¹) in a field-drained system with a topsoil clay content of ~10%. While this is not a complete review, annual sediment fluxes in field drained systems are clearly highly spatially variable, over several orders of magnitude. We hypothesised that the magnitude of the sediment flux related to the clay content of the soil. We therefore set the annual sediment flux in D1 to 0.03 kg m⁻² a⁻¹ and set the flux in D2 to the same value, since the D2 topsoil also has a clay content of ~50% (Table 1). For D3, where the topsoil clay content is <5%, we set the flux to 0.0003 kg m⁻² a⁻¹ and for D4 to D6, with topsoil clay varying from ~10–30% we set the flux to 0.003 kg m⁻² a⁻¹.

For the R scenarios the PRZM model (Carousel et al., 2003) was used to predict soil hydrology (surface runoff, vertical drainage at 5cm, 15cm and 30cm, and percolation

at the base of the soil profile) using the meteorological, soil and crop parameters provided by FOCUS (FOCUS, 2001). Annual volumes of water were computed by averaging the model predictions based on the multi-year input datasets provided in FOCUS. For setup and the 1745–1749 period the surface runoff was assumed to be 10% of the modelled annual mean, with the remaining water being routed into the 5–15cm layer. The annual pattern in surface runoff from the 0–5cm layer was obtained from PRZM outputs, from the daily volumes of surface runoff for a one year simulation period.

Table 2. Hydrological and erosion characteristics of the FOCUS scenarios.

Scenario code	Scenario location	Annual drainflow mm	Annual surface runoff mm	Annual baseflow mm	Annual erosion 0-5 cm layer kg m ⁻²
D1	Lanna, Sweden	191	0	12.1	0.03
D2	Brimstone, UK	298	0	0.22	0.03
D3	Vredepeel, Netherlands	331	0	0.38	0.0003
D4	Skousbo, Denmark	145	0	38.8	0.003
D5	La Jaillerie, France	195	0	27.1	0.003
D6	Vayia Thiva, Greece	199	0	67.7	0.003
R1	Weiherbach, Germany	–	44	70.1	0.079
R2	Valadares, Portugal	–	284	102	0.839
R3	Ozzabi, Italy	–	93	27.8	0.316
R4	Roujan, France	–	149	70.4	0.387

Annual topsoil erosion in the R scenarios was also obtained from PRZM outputs, by averaging annual predictions of surface erosion from the multi-year simulation period. The values used were 790, 8390, 3160 and 3870 kg ha⁻¹ a⁻¹ for R1–R4 respectively (0.079, 0.839, 0.316 and 0.387 kg m⁻² a⁻¹).

Crops and soil management

Simulations were done using winter wheat as a crop type in all scenarios except R2, where maize was used instead. Uptake of zinc by wheat and maize was computed from the expressions of de Vries et al. (2004), where the Zn content of crops is modelled as a function of the soil total metal, the soil pH (KCl extraction; pH_{KCl}), and the soil organic matter and clay contents. The expressions were adjusted to allow prediction on the basis of pH_{ss} rather than pH_{KCl}.

Tillage of the top horizon (0–15cm) was simulated for all the scenarios after 1750. The effect of tillage is to homogenise the properties (including metal contents) of the two layers representing this depth of topsoil.

Surface water setup

The FOCUS scenarios can have one of three types of waterbody. In all cases waterbodies were simulated using a single reach:

- streams drain a catchment area of 100ha. We set the reach length to 100m, depth 0.3m and width 1m.
- ditches drain a catchment area of 3ha and have the same dimensions as the stream.
- ponds drain a catchment area of 0.45ha and are 30m wide, 30 long and 1m deep.

We set the total sediment depth to 5cm with a 2cm upper layer. Initial masses of fine bottom sediment were set to 5 kg m⁻² for streams and ditches and 20 kg m⁻² for ponds. The fine sediment settling velocity was set to 1m d⁻¹ and the resuspension parameters A , μ and Q_{thr} were set to 10 kg m⁻³ s, unity, and 0.001m³ s⁻¹ respectively, except in ponds where A was set to zero to prevent any fine sediment resuspension. The bedload shift coefficient m was set to 0.002 m d⁻¹ in ditches and streams and to zero in ponds. The bioturbation coefficient k_{bio} was set to 0.001 kg² m⁻⁴ d⁻¹ in all scenarios.

Surface water chemistry was estimated as described in Monteiro et al. (2010). The organic matter content of SPM and bottom sediment was set to 10%. The acid–volatile sulphide (AVS) concentration in the lower sediment layer was set to 0.63 $\mu\text{mol g}^{-1}$. This is the median value obtained from a study of small streams across Europe by Burton et al. (2007). Sediment pH and major ion concentrations were set equal to the concentrations in surface water. Sediment Al and FeIII concentrations were computed assuming equilibrium with their hydroxides. The DOC concentration was set to 10 mg dm⁻³ in all scenarios. This concentration differs from that in the surface waters, on the assumption that sediment DOC concentration is buffered by generation of DOC within the sediment due to OM decomposition.

Risk assessment

We have assessed ecological risks by comparison of Predicted Environmental Concentrations (PEC; i.e. the model predictions) and Predicted No-Effect Concentrations (PNECs) in soil, surface waters and sediments. We have used the PNECs computed by Monteiro et al. (2010) in order to directly compare between the predictions of the IDMM-ag v2.0 and the older version of the IDMM used in that work. The PEC values used are given in Table 3.

Table 3. Predicted No-Effect Concentrations used for risk assessment.

	Soil $\mu\text{g g}^{-1}$	Copper Water $\mu\text{g dm}^{-3}$	Sediment $\mu\text{g g}^{-1}$	Soil $\mu\text{g g}^{-1}$	Zinc Water $\mu\text{g dm}^{-3}$	Sediment ^a $\mu\text{g g}^{-1}$
D1	139	30.1	87	123	11.4	70
D2	157	1.9	87	331	13.7	121
D3	55	17.4	87	131	30.3	74
D4	67	47.0	87	121	57.9	63
D5	97	4.1	87	152	14.3	77
D6	94	1.3	87	296	8.5	129
R1	64	3.0	87	201	8.4	84
R2	98	4.0	87	208	12.9	138
R3	90	2.4	87	325	11.0	116
R4	62	4.1	87	336	11.9	150

^a Total zinc PNEC, computed by summing added PNEC of 49 $\mu\text{g/g}$ and the predicted PEC under pristine (steady state) conditions.

Assessment of sediment risks is done by taking the PEC to be the concentration of labile metal less the concentration bound to AVS. We will term this the ‘SEM-AVS equivalent¹’ metal since . While the sediment PNECs are expressed as total metal, comparison with the SEM-AVS equivalent metal is valid because sediment toxicity testing is typically done by spiking with labile metal and testing on a short time, such that total concentration \approx labile concentration.

The PEC is computed for the whole depth of sediment, covering both the oxic layer (where AVS=0) and the anoxic layer (where AVS may be > 0):

$$\text{PEC}_{\text{SEM-AVS}} = 0.4 \cdot M_{\text{lab,oxic}} + 0.6 \cdot M_{\text{SEM-AVS,anoxic}}$$

where $M_{\text{lab,oxic}}$ is the labile metal concentration in the oxic layer and $M_{\text{SEM-AVS,anoxic}}$ is the ‘SEM-AVS equivalent’ metal in the anoxic layer, taken to be the sum of all WHAM-computed species except precipitated sulphides.

4. Results and Discussion

Predicted concentrations of copper and zinc in topsoils, surface waters and sediment are given in Appendix 1. Predictions were done both with an enrichment factor (f_e) for topsoil erosion of three, and without an enrichment factor. Topsoil concentrations of copper are generally similar to those in Monteiro et al. (2010), while topsoil concentrations of zinc are typically somewhat higher, but less variable than previously predicted.

¹ SEM = simultaneously extracted metal, that metal extracted in a 0.1M HCl extraction. This comprises porewater+adsorbed (i.e. labile) and SEM-bound metal. The term SEM-AVS refers to the SEM corrected for metal bound to AVS.

Figure 9 presents examples of changes in the percentage labile metal in topsoil for D6 (topsoil pH 6.0) and R4 (topsoil pH 7.6). In both cases the percentage of labile metal increases with time and cumulative input, particularly after 1950 and the onset of manure-associated inputs. The proportional increase is linked to the rate of aging (which is higher at higher pH). On the other hand, the absolute proportions are related to the total soil concentration under pristine conditions (which is specified in inputs to match ambient present day concentrations) and to the pristine labile concentration (which is a function of the soil chemistry and the hydrology under pristine conditions). It should be noted that the absolute percentages of labile metal should be lower than those that are observed in short-term aging experiments using metal salt spikes, where the measurements are of the aged state of the added metal only.

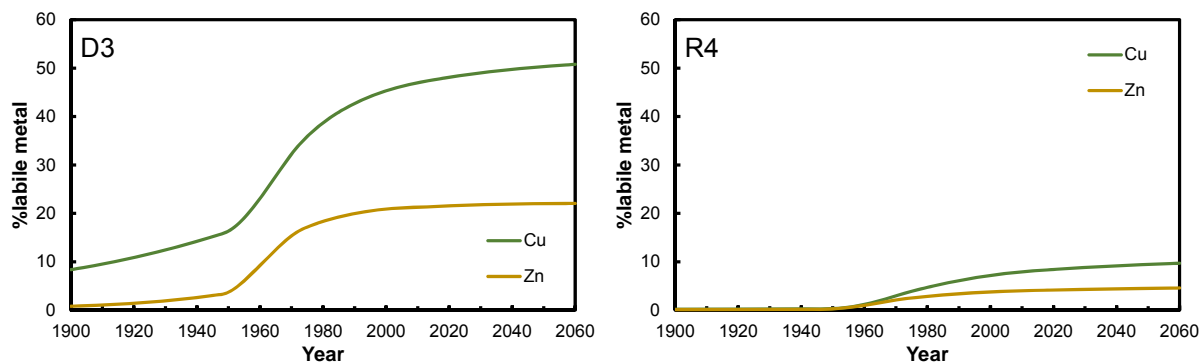


Figure 9. Examples of the change in proportions of copper and zinc predicted to be in labile form in the 0-30cm soil layer.

Surface water dissolved copper concentrations are generally higher in the D scenarios but lower in the R scenarios compared to the predictions of Monteiro et al. (2010). There are a number of possible reasons for these differences. The most important of these is the explicit modelling of surface water dynamics in this version of the model compared to the approach previously taken. Furthermore, the parameters used for partitioning of metals between the soil solids and the porewater have been updated, which is likely to result in different predictions of porewater concentrations and thus different fluxes of metal into the surface waters. It is notable that this version of the model predicts a greater range of surface water copper concentrations than seen previously through taking into better account the varying dynamics of the different surface water systems. This can be seen, for example, by considering the paired pond-stream scenarios (D4, D5 and R1) where the dissolved copper in ponds is consistently higher than in streams. This is due to the differing residence times of water in the two types of waterbody (Table 4) – in streams, water and dissolved metal coming from soilflow passes through the waterbody more rapidly than it does in ponds, and thus makes a lesser contribution to the annual time-averaged dissolved copper.

Of particular note are the very low dissolved copper concentrations predicted for the R stream scenarios. This is likely to be due to the different approach taken to estimating the baseflow concentrations of metals in this version of the model. Whereas in the approach of Monteiro et al. (2010) the baseflow metal concentrations were specified and based on ambient observed concentrations, in this version of the model concentrations are explicitly simulated and are generally lower than the previously used values. The hydrology of the R stream scenarios, with the number of days in a year having soilflow low compared to the D stream scenarios, also contributes to the

prediction of the low concentrations by resulting in a shorter time period per year during which soilflow-derived copper contributes to the annual time-averaged concentration.

Table 4. Bottom sediment masses, annual sediment deposition and bottom sediment residence times for the scenario surface waters.

SCENARIO CODE	SEDIMENT MASS KG	ANNUAL DEPOSITION KG	RESIDENCE TIME YR
D1 DITCH	500	728	0.69
D1 STREAM	500	2140	0.23
D2 DITCH	500	682	0.73
D2 STREAM	500	1920	0.26
D3 DITCH	500	8.5	58.8
D4 POND	18000	104	173
D4 STREAM	500	321	1.56
D5 POND	18000	103	175
D5 STREAM	500	201	2.49
D6 DITCH	500	66.6	7.51
R1 POND	18000	2720	6.62
R1 STREAM	500	6000	0.08
R2 STREAM	500	25100	0.02
R3 STREAM	500	8210	0.06
R4 STREAM	500	4620	0.11

Dissolved zinc concentrations are largely lower than previously modelled, with the exceptions of the D2 ditch and D5 pond scenarios. The overall variability in concentrations is lower but this is largely due to scenario D3, which as in Monteiro et al. (2010) has the highest predicted dissolved zinc concentrations. Some considerable differences in predicted concentrations are seen – as with copper, concentrations in the stream scenarios are consistently lower than previously, as a result of the different approach to modelling the background concentration, and also to some extent due to the explicit modelling of waterbody dynamics. Concentrations in the ditch scenarios are generally somewhat lower than previously estimated, except for D2. This is most likely being driven by lower background concentrations, which except for D2 dominates over the effect of taking waterbody dynamics into account (which would tend to increase the modelled concentrations by taking the residence time of zinc in the system into account).

Sediment total concentrations of metals are generally lower than previously simulated, particularly for ponds. This latter effect is due to the greater ‘dilution’ of depositing sediment by the sediment already present. The pond waterbody has a total bottom fine mass of 18000 kg, compared to 500kg for the stream and ditch, so the residence times of fine sediment in the active layer are generally higher than for the other water bodies. Additionally, ponds have the smallest catchment area of the waterbodies so the absolute flux of incoming sediments tends to be smaller, which dominates over the greater relative removal of suspended sediment due to the longer residence time of water in the pond. The exception to this general rule is R1, where the rate of sediment input and deposition results in similar sediment concentrations to the corresponding stream scenario. SEM–AVS equivalent concentrations, used here for risk assessment, were not computed in Monteiro et al. (2010) so no comparison can be made.

Potential risks, expressed as the risk assessment ratio, RAR (RAR = PEC/PNEC) are shown in Table 5 to Table 10. There is no potential risk predicted for the 0-30cm topsoil

layer in any scenario, which agrees with the findings of Monteiro et al. (2010) (Figure 10). The predicted RARs for zinc are generally somewhat higher than those of Monteiro et al. (2010) (i.e. predicted concentrations are somewhat higher). Exceedences of surface water PNECs are confined to D2, D5 and D6 for copper, and to D3 for zinc (Figure 11). In contrast, Monteiro et al. (2010) computed no exceedences for copper, and exceedences in D3 and R2 for zinc. For copper, this is most likely related to the relatively low PNECs in scenarios D2 and D3. For zinc, the PNEC in D3 is relatively high at $>30 \mu\text{g dm}^{-3}$, however the scenario has by far the highest predicted dissolved zinc concentrations (Table A7). It is likely that with the exception of D3, the differences seen in PECs and thus RARs are due to the explicit modelling of the surface water dynamics. In D3, by contrast, the predictions appear to be controlled by the high leaching rate of zinc from this acid sandy soil, which overrides the influence of the surface water dynamics. In general, the updated model gives the greatest difference in predicted RAR, compared to Monteiro et al. (2010), for copper in surface waters. In Monteiro et al. (2010) RARs for different waterbodies with the same soil scenario gave similar predictions, whereas here, with the exception of D2, the stream scenarios give substantially lower RARs than either the paired ditch or pond scenario, or the predictions of Monteiro et al. (2010). In the extreme case, the PECs predicted in R2 are substantially lower than those of Monteiro et al. (2010) (e.g. in 2060, $34.2 \mu\text{g dm}^{-3}$ from Monteiro et al. (2010), $0.27 \mu\text{g dm}^{-3}$ in this study). This again demonstrates the influence of explicitly considering the surface water dynamics in modelling.

Table 5. Risk assessment ratios (RARs) for copper in topsoil.

Scenario code	RAR 2000	RAR 2010	RAR 2020	RAR 2030	RAR 2060
D1	0.08	0.09	0.09	0.10	0.13
D2	0.13	0.14	0.14	0.15	0.18
D3	0.28	0.31	0.33	0.35	0.42
D4	0.17	0.19	0.20	0.22	0.26
D5	0.13	0.15	0.15	0.16	0.19
D6	0.35	0.37	0.38	0.39	0.43
R1	0.26	0.28	0.29	0.31	0.36
R2	0.13	0.14	0.14	0.14	0.15
R3	0.37	0.38	0.38	0.39	0.41
R4	0.49	0.50	0.51	0.52	0.54

Table 6. Risk assessment ratios (RARs) for zinc in topsoil.

Scenario code	RAR 2000	RAR 2010	RAR 2020	RAR 2030	RAR 2060
D1	0.48	0.54	0.60	0.65	0.82
D2	0.37	0.40	0.42	0.44	0.50
D3	0.54	0.60	0.65	0.71	0.86
D4	0.47	0.53	0.58	0.63	0.78
D5	0.42	0.46	0.49	0.53	0.64
D6	0.41	0.43	0.46	0.48	0.55
R1	0.46	0.49	0.52	0.56	0.65
R2	0.44	0.45	0.46	0.47	0.48
R3	0.37	0.39	0.40	0.42	0.46
R4	0.40	0.42	0.43	0.44	0.47

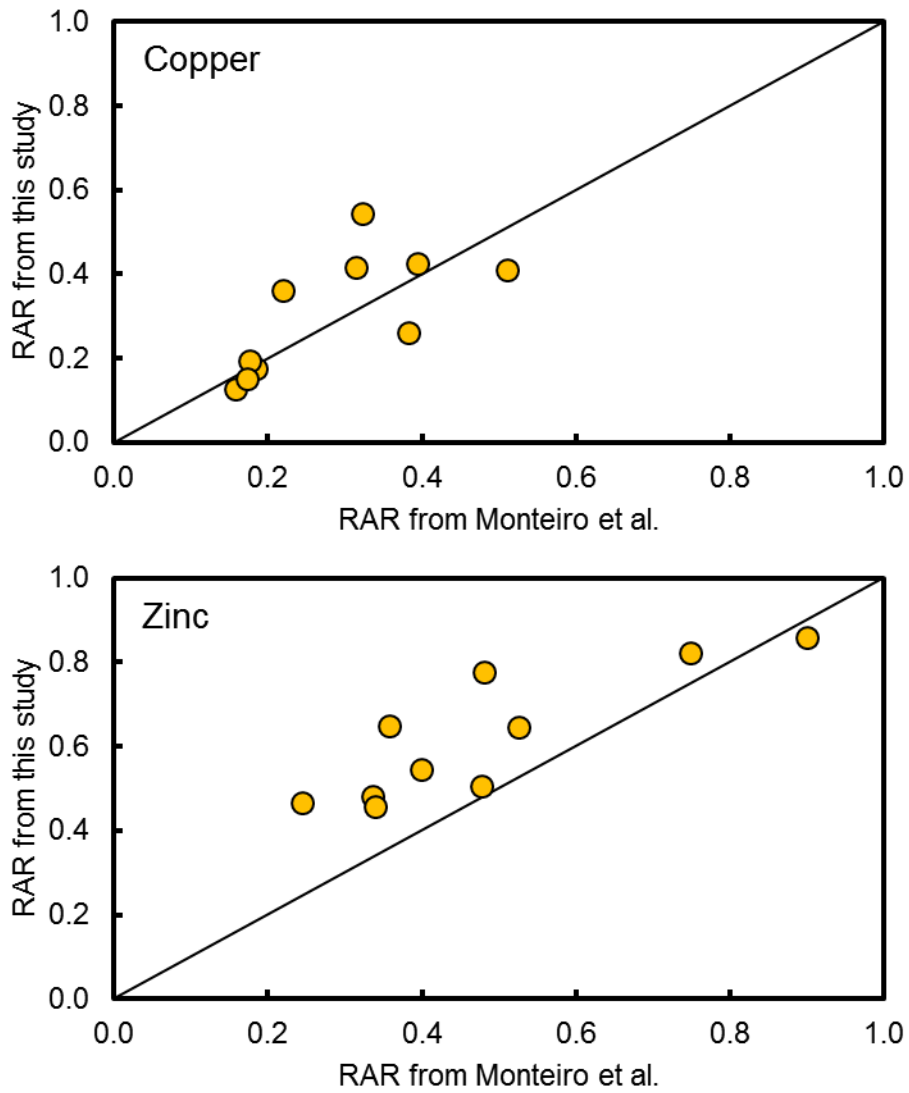


Figure 10. Comparison of topsoil RARs derived from the modelling of Monteiro et al. (2010) and that in the present study. The black line is the 1:1 line and the red dotted lines show the potential risk threshold of RAR = 1.

Table 7. Risk assessment ratios (RARs) for copper in surface water.

Scenario code	RAR 2000	RAR 2010	RAR 2020	RAR 2030	RAR 2060
D1 stream	0.01	0.01	0.01	0.01	0.01
D1 ditch	0.09	0.11	0.12	0.13	0.15
D2 stream	1.19	1.30	1.39	1.48	1.71
D2 ditch	3.73	4.09	4.37	4.63	5.32
D3 ditch	0.54	0.61	0.67	0.72	0.86
D4 stream	0.00	0.01	0.01	0.01	0.01
D4 pond	0.13	0.15	0.17	0.18	0.22
D5 stream	0.03	0.04	0.04	0.04	0.05
D5 pond	1.33	1.55	1.74	1.91	2.36
D6 ditch	1.10	1.27	1.42	1.55	1.89
R1 stream	0.01	0.01	0.01	0.01	0.01
R1 pond	0.30	0.34	0.38	0.41	0.49
R2 stream	0.00	0.00	0.00	0.00	0.00
R3 stream	0.03	0.03	0.03	0.03	0.03
R4 stream	0.01	0.01	0.01	0.01	0.01

Table 8. Risk assessment ratios (RARs) for zinc in surface water.

Scenario code	RAR 2000	RAR 2010	RAR 2020	RAR 2030	RAR 2060
D1 stream	0.03	0.04	0.04	0.04	0.05
D1 ditch	0.26	0.30	0.34	0.37	0.47
D2 stream	0.22	0.25	0.28	0.31	0.38
D2 ditch	0.49	0.56	0.63	0.69	0.87
D3 ditch	1.24	1.45	1.63	1.81	2.28
D4 stream	0.00	0.00	0.01	0.01	0.01
D4 pond	0.10	0.12	0.14	0.16	0.20
D5 stream	0.01	0.01	0.02	0.02	0.02
D5 pond	0.42	0.51	0.58	0.65	0.85
D6 ditch	0.19	0.22	0.25	0.27	0.35
R1 stream	0.01	0.01	0.01	0.01	0.01
R1 pond	0.33	0.39	0.44	0.48	0.62
R2 stream	0.01	0.02	0.02	0.02	0.03
R3 stream	0.01	0.01	0.01	0.01	0.01
R4 stream	0.00	0.00	0.00	0.00	0.00

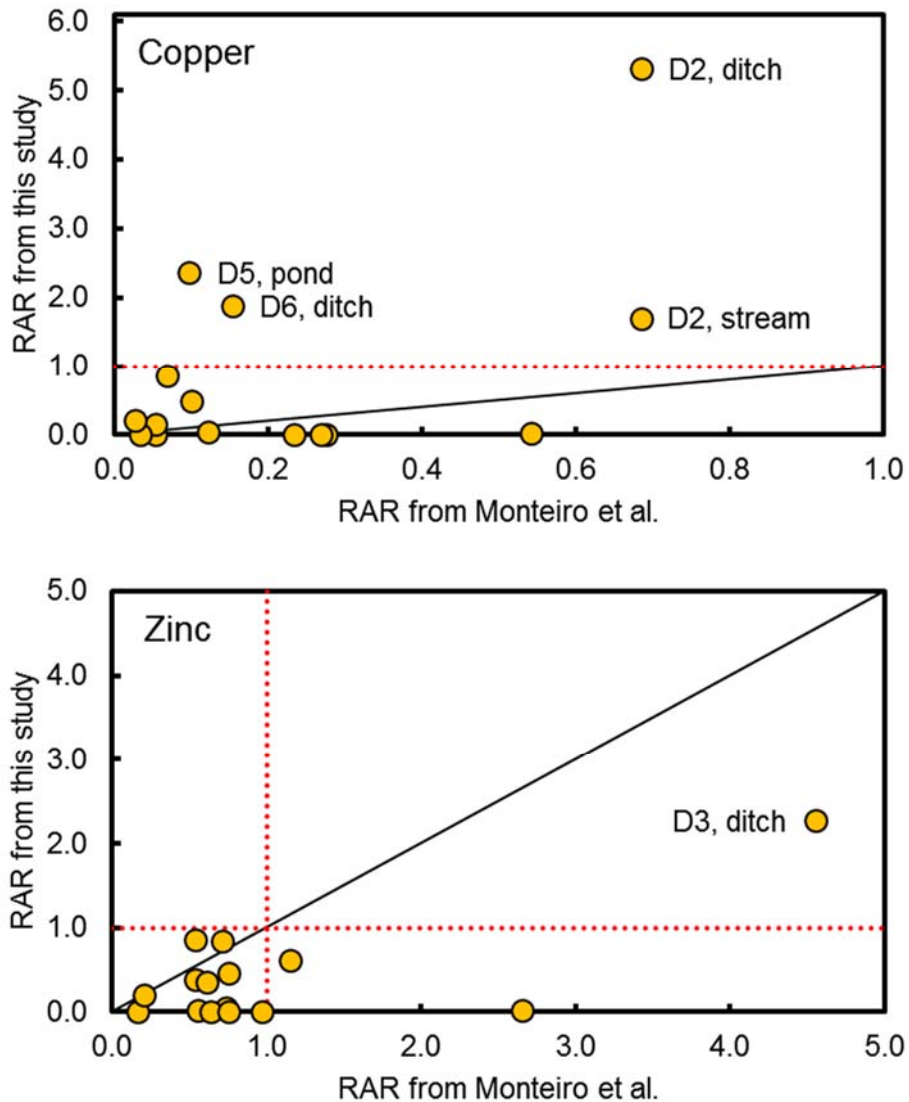


Figure 11. Comparison of surface water RARs derived from the modelling of Monteiro et al. (2010) and that in the present study. The black line is the 1:1 line and the red dotted lines show the potential risk threshold of RAR = 1.

In contrast to Monteiro et al. (2010) predicted exceedence of sediment PNECs is confined to zinc in D3, where exceedence is predicted in 2048. This is due largely to the consideration of SEM–AVS equivalent metal as the PNEC. The role of AVS in further reducing the PNECs is predicted to be most important for copper; in 2020 the mean RCR is 0.12 in the presence of 0.63 $\mu\text{mol/g}$ AVS and 0.29 in the absence of AVS, while for zinc the mean RCR is 0.39 in the presence of 0.63 $\mu\text{mol/g}$ AVS and 0.47 in the absence of AVS. This reflects the predicted ability of copper to preferentially form a sulphide precipitate. If the available AVS to bind both copper and zinc is exceeded as sediment metal loadings increase, copper will then displace zinc from the AVS–bound pool and gradually reduce the predicted AVS–bound zinc. In scenarios D2, D3, D6 and R1 pond, by 2060 there is predicted to be no AVS–bound zinc due to copper binding all the AVS.

Modelling sediment accumulation assuming no enrichment of eroded soil in metal predicts lower RARs, as would be expected: for example, the RARs for copper in 2060 are between 1.4 and 3.6 times lower than those predicted assuming enrichment, and those for zinc are between 2.5 and 7.1 times lower. No risks to 2060 are predicted when modelling without enrichment.

Table 9. Risk assessment ratios (RARs) for copper in sediment. Values not in brackets refer to an enrichment factor of three, values in brackets refer to an enrichment factor of unity.

Scenario code	RAR 2000	RAR 2010	RAR 2020	RAR 2030	RAR 2060
D1 STREAM	0.09 (0.03)	0.11 (0.04)	0.12 (0.04)	0.13 (0.05)	0.17 (0.06)
D1 DITCH	0.09 (0.03)	0.11 (0.04)	0.12 (0.04)	0.13 (0.05)	0.17 (0.06)
D2 STREAM	0.15 (0.05)	0.16 (0.06)	0.18 (0.06)	0.20 (0.07)	0.30 (0.08)
D2 DITCH	0.16 (0.07)	0.18 (0.07)	0.20 (0.08)	0.24 (0.09)	0.34 (0.10)
D3 DITCH	0.09 (0.06)	0.12 (0.08)	0.15 (0.09)	0.18 (0.11)	0.36 (0.15)
D4 STREAM	0.08 (0.03)	0.09 (0.03)	0.10 (0.04)	0.12 (0.04)	0.15 (0.05)
D4 POND	0.02 (0.01)	0.03 (0.01)	0.04 (0.02)	0.05 (0.02)	0.09 (0.04)
D5 STREAM	0.08 (0.03)	0.09 (0.04)	0.11 (0.04)	0.12 (0.05)	0.16 (0.06)
D5 POND	0.04 (0.03)	0.06 (0.04)	0.08 (0.06)	0.10 (0.07)	0.16 (0.11)
D6 DITCH	0.11 (0.07)	0.14 (0.08)	0.16 (0.10)	0.17 (0.10)	0.27 (0.13)
R1 STREAM	0.09 (0.03)	0.11 (0.04)	0.12 (0.04)	0.13 (0.05)	0.16 (0.06)
R1 POND	0.10 (0.05)	0.12 (0.05)	0.13 (0.06)	0.15 (0.07)	0.19 (0.08)
R2 STREAM	0.07 (0.03)	0.08 (0.03)	0.08 (0.04)	0.09 (0.04)	0.09 (0.04)
R3 STREAM	0.11 (0.04)	0.12 (0.04)	0.12 (0.05)	0.13 (0.05)	0.15 (0.06)
R4 STREAM	0.06 (0.02)	0.07 (0.03)	0.08 (0.03)	0.08 (0.03)	0.10 (0.04)

Table 10. Risk assessment ratios (RARs) for zinc in sediment. Values not in brackets refer to an enrichment factor of three, values in brackets refer to an enrichment factor of unity.

Scenario code	RAR 2000	RAR 2010	RAR 2020	RAR 2030	RAR 2060
D1 STREAM	0.39 (0.08)	0.51 (0.09)	0.61 (0.10)	0.71 (0.11)	0.99 (0.14)
D1 DITCH	0.38 (0.08)	0.50 (0.09)	0.61 (0.10)	0.70 (0.11)	0.98 (0.14)
D2 STREAM	0.34 (0.05)	0.42 (0.06)	0.48 (0.07)	0.53 (0.07)	0.65 (0.11)
D2 DITCH	0.35 (0.05)	0.42 (0.06)	0.47 (0.07)	0.52 (0.07)	0.64 (0.13)
D3 DITCH	0.20 (0.05)	0.38 (0.07)	0.57 (0.09)	0.75 (0.14)	1.17 (0.36)
D4 STREAM	0.29 (0.07)	0.42 (0.08)	0.52 (0.10)	0.62 (0.11)	0.91 (0.14)
D4 POND	0.07 (0.03)	0.09 (0.04)	0.12 (0.05)	0.14 (0.06)	0.22 (0.09)
D5 STREAM	0.23 (0.06)	0.34 (0.07)	0.43 (0.08)	0.52 (0.09)	0.77 (0.11)
D5 POND	0.06 (0.03)	0.08 (0.03)	0.10 (0.04)	0.12 (0.05)	0.20 (0.08)
D6 DITCH	0.14 (0.03)	0.22 (0.04)	0.28 (0.05)	0.34 (0.05)	0.47 (0.11)
R1 STREAM	0.32 (0.06)	0.41 (0.07)	0.49 (0.08)	0.57 (0.09)	0.77 (0.11)
R1 POND	0.29 (0.07)	0.40 (0.08)	0.49 (0.09)	0.57 (0.10)	0.79 (0.15)
R2 STREAM	0.22 (0.05)	0.24 (0.05)	0.24 (0.06)	0.24 (0.06)	0.23 (0.06)
R3 STREAM	0.24 (0.05)	0.29 (0.05)	0.33 (0.06)	0.36 (0.06)	0.44 (0.08)
R4 STREAM	0.07 (0.02)	0.09 (0.03)	0.12 (0.03)	0.14 (0.04)	0.20 (0.04)

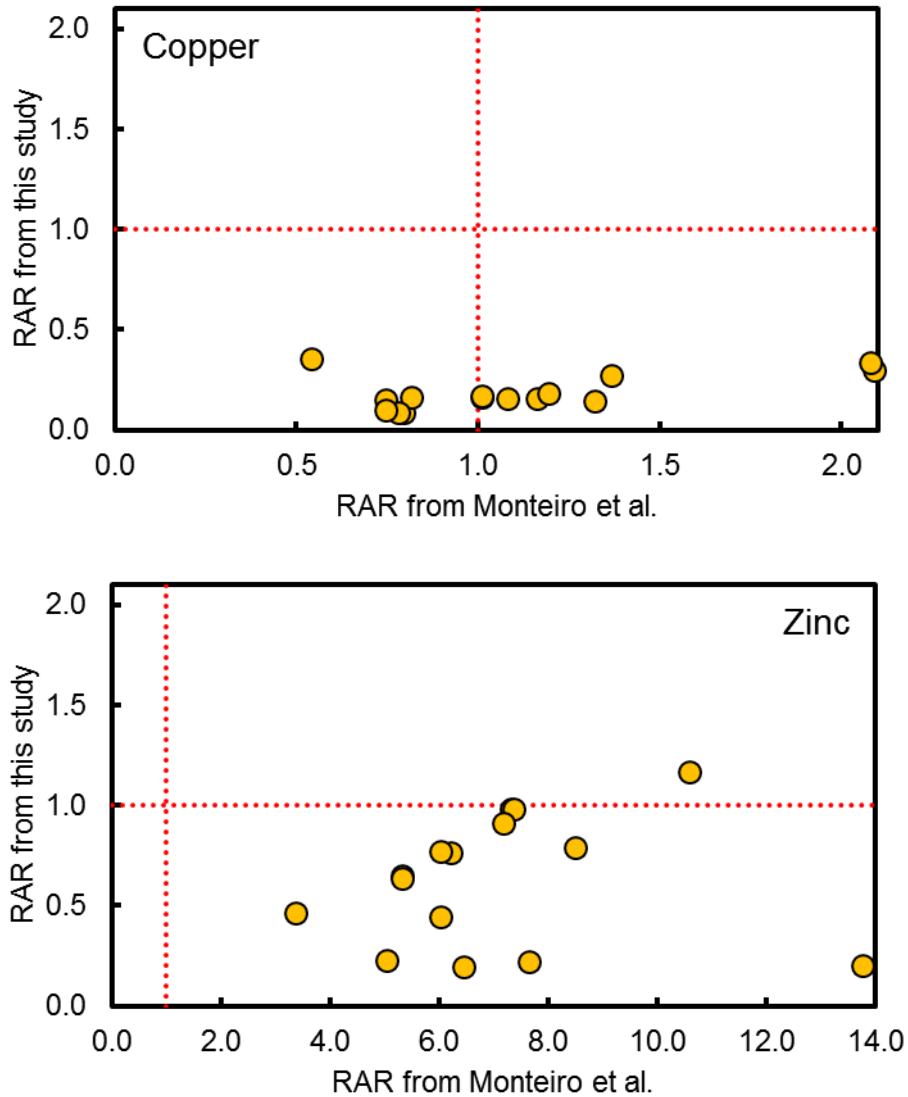


Figure 12. Comparison of sediment RARs derived from the modelling of Monteiro et al. (2010) (using total metal PECs) and those derived in the present study (using SEM-AVS equivalent PECs). The black line is the 1:1 line and the red dotted lines show the potential risk threshold of RAR = 1.

The choice of enrichment factor is key in determining the simulated sediment concentrations. **Error! Reference source not found.** shows predictions of labile sediment metal concentrations in the D2, stream and D5, pond scenarios assuming no enrichment and an enrichment factor of three, and with an enrichment factor of three in the absence of AVS, for reference. Predicted labile topsoil concentrations for 0-15cm are also shown.

The predictions for D2, stream show a strong effect of the enrichment factor on sediment metal and also illustrate the effect of AVS. If neither enrichment nor AVS binding are simulated, the SEM-AVS equivalent concentrations are similar to the labile metal concentrations in the topsoil for the same year. This results from the rapid turnover of sediment (Table 4) coupled with only a small redistribution of labile metal between the dissolved and adsorbed phases prior to sediment settling. With enrichment, SEM-AVS equivalent concentrations are ~3 times higher. The predictions with AVS show the effects on reducing the SEM-AVS equivalent concentrations, but also the effects of exceeding the binding capacity of the AVS and the contrasting

effects this has on copper and zinc. In the absence of enrichment, both copper and zinc concentrations are consistently reduced. A change in the zinc trend can be seen around 2040; this marks the point at which the capacity of the AVS to bind both metals is reached. Beyond this point additional copper removes zinc from the AVS-bound pool, resulting in a higher rate of increase in zinc concentration over time. In the predictions where an enrichment factor of three is used, the capacity of AVS to bind both copper and zinc is reached in the 1970s, while in the 2020s the capacity to bind copper alone is exceeded. In the charts, these points can be clearly seen as inflections (changes in time trend), firstly for zinc and secondly for copper. Furthermore, at the point in time where the capacity of AVS to bind copper is reached, the amount of AVS-bound zinc becomes zero.

Similar trends are seen in the D5, pond scenario, but because of the longer sediment residence time of fine sediment in the active layer of the pond, predicted concentrations are lower than those in the 0-15cm soil, even if an enrichment factor is applied. Because of this, accumulation rates and thus concentrations are lower, and the capacity for AVS to bind metals is not exceeded. Simulating bioturbation in the sediment is important here; if it were not simulated then there would be a greater buildup of metal in the upper sediment layer with higher resulting concentrations. Over time, bioturbation mixes some of the freshly deposited, more contaminated sediment into the lower layer where it is subject to burial.

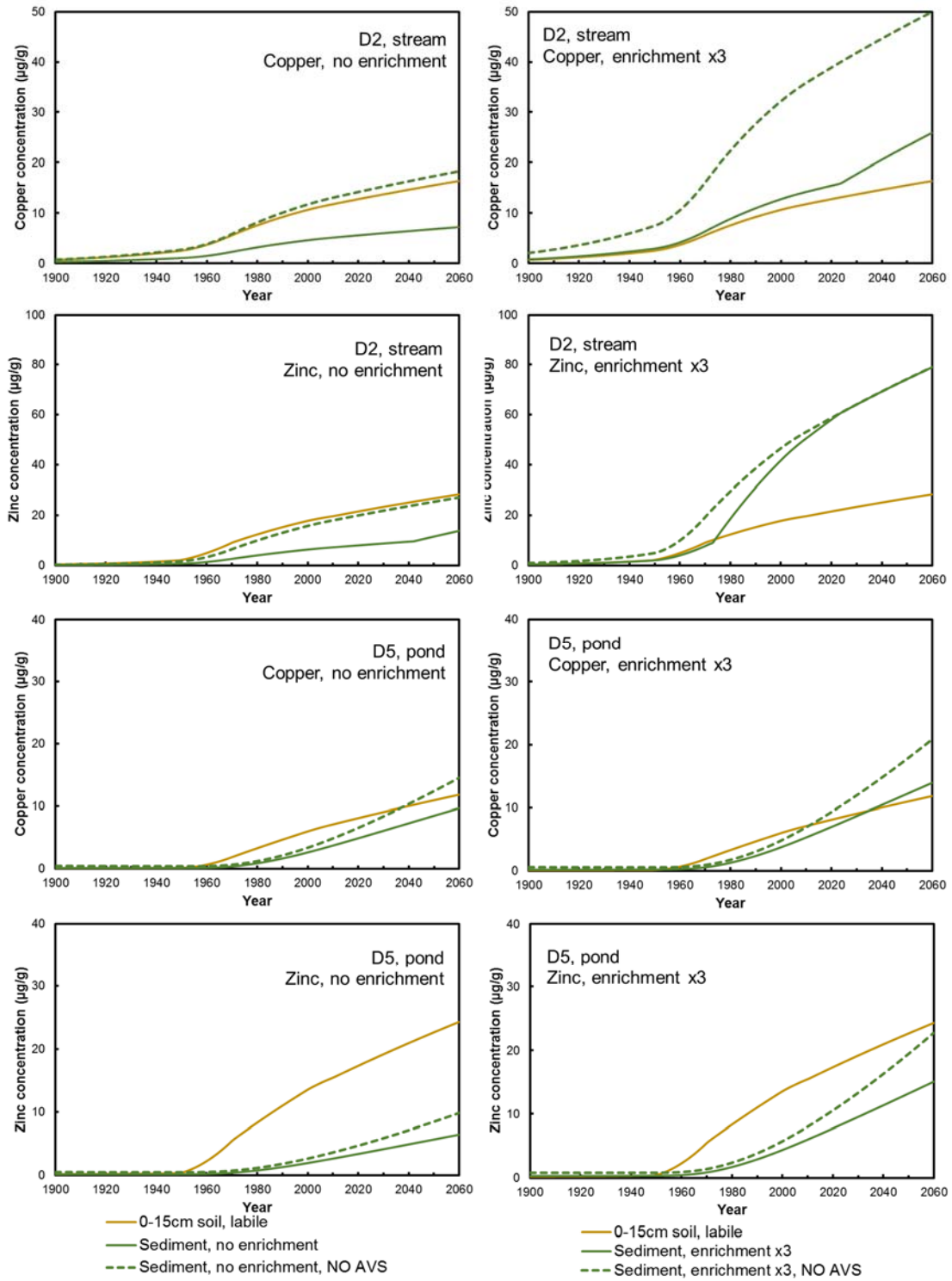


Figure 13. Examples showing the effect of the choice of enrichment factor on the predicted sediment 'SEM-AVS equivalent' metal concentrations. Predictions for D2, stream and D5, pond for 1900 to 2060.

More research is needed on the causes of the apparent enrichment of metals in eroded soil relative to the bulk soil. In particular, it needs to be better established to what extent observed enrichment reflects a process of erosional selection of particles relatively rich in metals, as opposed to an artefact caused by vertical heterogeneity of metal concentrations within sampled topsoil.

The presence of AVS in the lower layer of the bottom sediment has an important effect on limiting the concentrations of labile metals. Figure 15 shows this for the two scenarios with the highest and lowest predicted sediment metal concentrations, D2, stream and D5, pond respectively. The general pattern of predicted behaviour is for all labile copper and zinc in the sediment to be AVS-bound if the sum of their molar concentrations does not exceed that of AVS. As accumulation progresses, if the molar sum of metal concentrations exceeds the molar AVS concentration then the zinc concentration in excess of AVS is predicted to remain in labile form. If further accumulation then results in the molar concentration of copper exceeding AVS, then copper also appears in labile form. This can be seen in predicted labile metal concentrations for D2, stream. Here, the sediment residence time is short (< 1 year), the concentrations of labile metal in sediment are close to those in the depositing sediment, and the concentrations of total metal, and the sum of labile and AVS-bound metal, are similar in the two sediment layers. Copper and zinc accumulation in the lower sediment layer is sufficient that zinc starts to appear in labile form in the lower sediment in the 1970s, and copper around 2030. After the point at which labile zinc starts to appear, further accumulation of copper gradually reduces the concentration of AVS-bound zinc until the concentration of copper exceeds that of AVS in 2030. After this point, all the AVS is predicted to bind copper. There is no binding of AVS at all by zinc, and the labile concentrations in both sediment layers are predicted to be the same from this point onwards. Copper in the lower sediment layer is still predicted to be $>90\%$ AVS-bound in 2060. It is to be expected that further accumulation of copper will be predicted to be entirely in labile form, with the predicted AVS-bound concentration constant.

The D5, pond scenario presents a contrasting picture. The sediment residence time is relative long (>150 years) and so the combined copper and zinc accumulation to 2060 does not exhaust the available supply of AVS in the lower sediment layer. Hence the predicted labile concentrations of copper and zinc in the lower layer are consistently ~ 0 . Due to the long sediment residence time, the predicted labile metal concentrations in the upper layer are always higher than the AVS-bound concentrations in the lower layer, and binding of metals by AVS has a smaller relative effect on the labile concentrations in the whole sediment than it does in D2, stream.

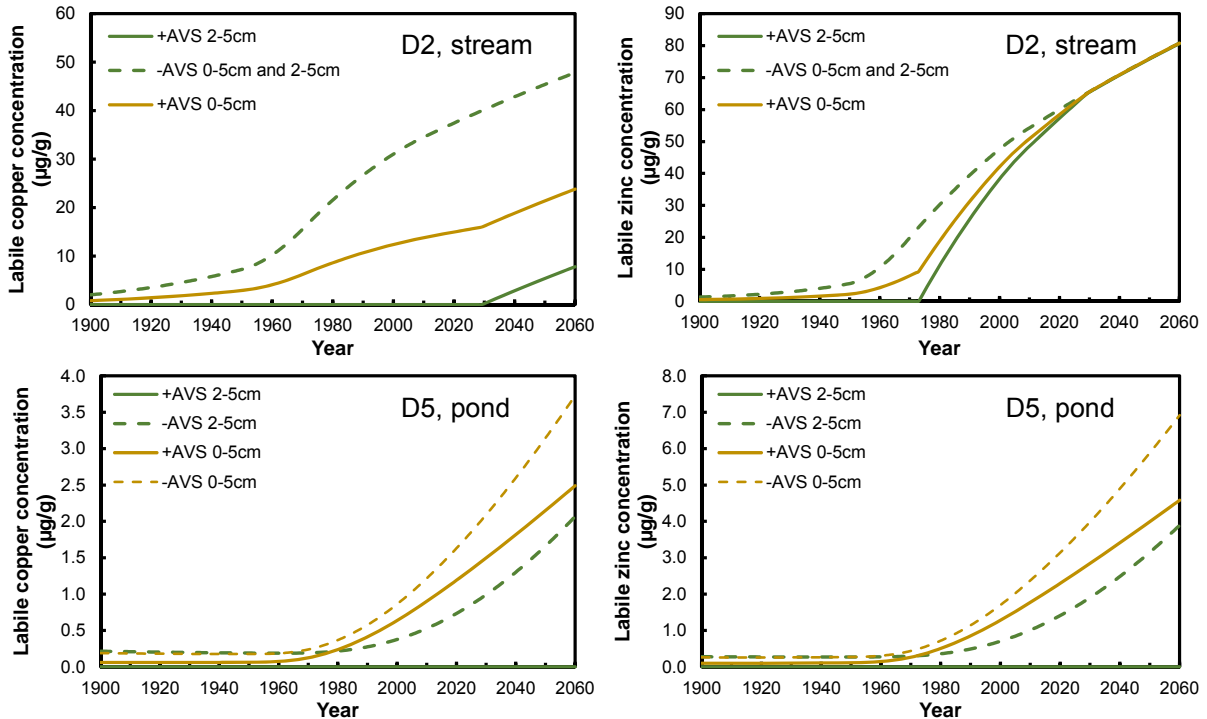


Figure 14. Examples of the influence of AVS on the predicted concentrations of labile metal in bottom sediments. Simulations labelled '+AVS' include $0.63 \mu\text{mol/g}$ AVS in the lower sediment layer. Simulations labelled '-AVS' have no AVS.

The D3, ditch scenario warrants mention as it represents relatively unusual physicochemical conditions. The location has a high water table and the annual pattern of water flow to field drains predicted by MACRO (Figure 15) is much less 'flashy' than for the other scenarios (cf. Figure 5). Flow via drains to surface water is predicted to occur every day, in contrast to the other scenarios. This means that the surface water dissolved metals concentrations in this scenario are always influenced by drainflow, which transports metal-enriched porewater from the uppermost soil layer into surface water. The result is that the predicted annual time-averaged metal concentrations in this scenario are higher than they would be if the annual drainflow pattern were more characteristic of that seen in the other scenarios. This is particularly seen in the high predicted concentrations of dissolved zinc in surface waters. Fluxes of zinc from the top soil layer are also influenced by its relatively low pH (6.0) compared to the other scenarios with the exception of R2.

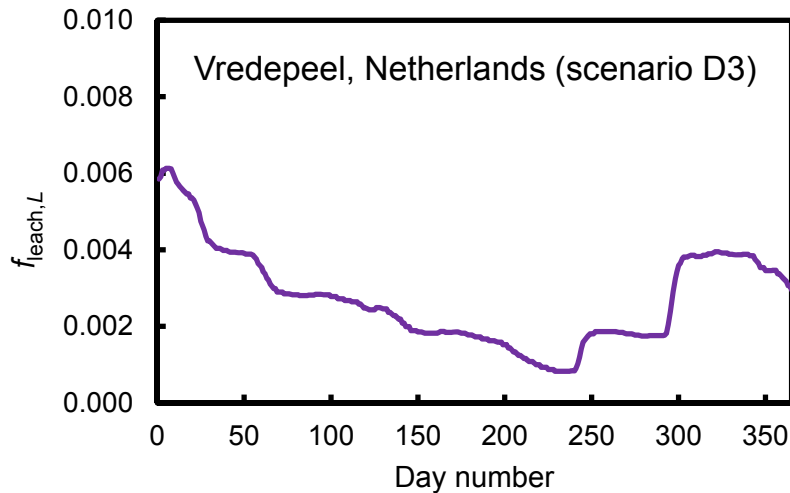


Figure 15. Annual pattern of daily $f_{\text{leach},L}$ values for scenario D3.

A key assumption in the modelling is that all the input metal is in labile form. This is a reasonable ‘worst case’ scenario if no information on the speciation of input metal is available. If metal lability in the inputs is significantly lower than 100% then this could have an important influence on predicted metal leaching to surface waters in dissolved form, and on the concentrations of labile metal in eroded soil eventually entering sediments. This may be particularly pertinent in the case of manure-associated inputs where the matrix may influence lability. Information on this is rather sparse, although Smolders et al. (2012) found some evidence that copper in manure had <100% lability. Such a factor could be important in determining long term metal dynamics and risks and warrants further investigation.

Field validation of the model predictions is clearly a priority. Validation along a long time series is unlikely to be feasible except in specific locations subject to long-term monitoring. Such monitoring is more likely to be focused on soil accumulation (e.g. Fan et al., 2008). We suggest, however, that a more important aspect of the model for priority testing is the transfer of metals to surface water and their subsequent behaviour in the water column and sediment. This is because accumulation in soils (at least of total metal) is so extensive, due to the highly particle-reactive nature of the metals, that it should be predominantly controlled by cumulative inputs. Except in a few well-monitored field experiments, past cumulative inputs are likely to be poorly known and thus prediction of present day concentrations would be highly dependent upon assumptions. On the other hand, present day metal transfers to surface waters will depend on the present day concentrations and speciation of metals in the soils and prediction of transfers to surface waters would be less dependent on estimation of past inputs, as long as robust information on present day concentrations and speciation in catchment soils were known or could be obtained. There have been past observational studies on metal transfers to surface waters from metal-contaminated agricultural soils (e.g. Xue et al., 2000; Banas et al., 2010) yet they typically focus on time periods of <1 year. Given that the IDMM-ag is designed for predictions on longer timescales, longer term studies of at least one year duration would be more useful to capture longer term metal fluxes into, through and out of agricultural systems. The importance of the enrichment factor, on the other hand, would be better examined across a range of topsoil types and hydrologies. There are clearly studies which show enrichment, however the degree to which it may vary in space and time, and the underlying mechanisms, remain somewhat unclear. Given that the enrichment factor has an

important influence on metal fluxes to surface water the ability to better assign values based on properties such as soil type would be an important refinement to the model.

5. Conclusions

- We applied an improved version of the IDMM (IDMM–ag) to scenarios of manure addition to soils first simulated by Monteiro et al. (2010) using an earlier version of the model. The major change between the model types is the explicit consideration of surface water dynamics and sediment accumulation in surface waters.
- The model produced estimates of topsoil copper and zinc concentrations broadly similar to those previously considered.
- Predicted surface water dissolved metal concentrations were more variable across scenarios, reflecting the importance of surface water dynamics in controlling annual average concentrations.
- Predicted sediment concentrations were generally lower than those previously modelled, reflecting the importance of explicitly modelling bottom sediment accumulation. Residence time of sediment within the ‘active’ bottom layer was key in controlling the build up of metals over time.
- Predicted risks were generally lower in this study, compared to that of Monteiro et al. (2010). There was a clear influence on RARs of taking the surface water dynamics into account. This was clearest for copper in surface waters, where predicted concentrations were far lower than previously computed in surface waters, with the exception of one scenario. Predicted sediment concentrations were generally lower than previously predicted, although in the case of zinc this still resulted in widespread predicted exceedence.
- The presence of acid–volatile sulphide was predicted to have a key influence on controlling concentrations of labile metals in bottom sediments, particularly in ponds, where metal accumulation was slower. In stream scenarios a greater likelihood exist of eventually exhausting the supply of AVS and thus the capacity to sequester incoming labile metal in a nonlabile form.
- Model testing against field data is a priority. In particular, long term monitoring of stream and sediment responses in contaminated catchments would allow testing of the surface water component of the model. Spatial assessment of the importance of poorly known variables, particularly the enrichment factor, would also improve the robustness of the model predictions.

6. References

Banas, D., Marin, B., Skraber, S., Chopin, E.I.B., Zanella, A. (2010). Copper mobilization affected by weather conditions in a stormwater detention system receiving runoff waters from vineyard soils (Champagne, France). *Environmental Pollution* 158: 476–482.

Burton, G.A., Green, A., Baudo, R., Forbes, V., Nguyen, L.T.H., Janssen, C.R., Kukkonen, J., Leppanen, M., Maltby, L., Soares, A.M.V.M., Kapo, K., Smith, P.,

Dunning, J. (2007). Characterizing sediment acid volatile sulfide concentrations in European streams. *Environmental Toxicology and Chemistry* 26: 1–12.

Carousel, R.F., Imhoff, J.C., Hummel, P.R., Cheplick, J.M., Donigian, A.S., Jr. (2003). PRZM-3: A model for predicting pesticide and nitrogen fate in the crop root and unsaturated soil zones: Users Manual for Release 3.12. Center for Exposure Assessment Modeling (CEAM), U.S. Environmental Protection Agency (USEPA), Athens, GA, U.S.A.

Crout, N.M.J., Tye, A.M., Zhang, H., McGrath, S.P., Young, S.D. (2006). Kinetics of metal fixation in soils: Measurement and modeling by isotopic dilution. *Environmental Toxicology and Chemistry* 25: 659–663.

European Commission, Health & Consumer Protection Directorate-General (2003a). Opinion of the Scientific Committee for Animal Nutrition on the use of copper in feedingstuffs. http://ec.europa.eu/food/fs/sc/scan/out115_en.pdf

European Commission, Health & Consumer Protection Directorate-General (2003b). Opinion of the Scientific Committee for Animal Nutrition on the use of zinc in feedingstuffs. http://ec.europa.eu/food/fs/sc/scan/out120_en.pdf

Fan, M.S., Zhao, F.J., Fairweather-Tait, S.J., Poulton, P.R., Dunham, S.J., McGrath, S.P. (2008). Evidence of decreasing mineral density in wheat grain over the last 160 years. *Journal of Trace Elements in Medicine and Biology* 22: 315–324.

FOCUS (2001). FOCUS Surface Water Scenarios in the EU Evaluation Process under 91/414/EEC. Report of the FOCUS Working Group on Surface Water Scenarios, EC Document Reference SANCO/4802/2001-rev.2. 245 pp.

Gregory, A. S.; Ritz, K.; McGrath, S. P.; Quinton, J. N.; Goulding, K. W. T.; Jones, R. J. A.; Harris, J. A.; Bol, R.; Wallace, P.; Pilgrim, E. S.; Whitmore, A. P. (2015). A review of the impacts of degradation threats on soil properties in the UK. *Soil Use and Management* 31: 1–15.

Groenenberg, J.E.; Römkens, P.F.A.M.; Comans, R.N.J.; Luster, J.; Pampura, T.; Shotbolt, L.; Tipping, E.; de Vries, W. (2010). Transfer functions for solid-solution partitioning of cadmium, copper, nickel, lead and zinc in soils: derivation of relationships for free metal ion activities and validation with independent data. *European Journal of Soil Science* 61: 58–73.

Larsbo, M., Jarvis, N. (2003). MACRO 5.0. A model of water flow and solute transport in macroporous soil. Technical description. Emergo 2003:5. Studies in the Biogeophysical Environment. Department of Soil Sciences, SLU, Uppsala, Sweden, 48 pp.

Lofts, S.; Tipping, E.; Lawlor, A.J.; Shotbolt, L. (2013). An intermediate complexity dynamic model for predicting accumulation of atmospherically-deposited metals (Ni, Cu, Zn, Cd, Pb) in catchment soils: 1400 to present. *Environmental Pollution* 180: 236–245.

Ma, Y.B., Lombi, E., Oliver, I.W., Nolan, A.L., McLaughlin, M.J. (2006). Long-term aging of copper added to soils. *Environmental Science & Technology* 2006, 40, (20), 6310-6317.

Monteiro, S.; Lofts, S.; Boxall, A.B.A. (2010). Pre-Assessment of Environmental Impact of Zinc and Copper Used in Animal Nutrition. Parma, Italy, European Food Safety Authority, 325pp.

Nriagu, J.O. (1996). A history of global metal pollution. *Science* 272: 223.

Quinton, J. N.; Catt, J. A. (2007). Enrichment of heavy metals in sediment resulting from soil erosion on agricultural fields. *Environmental Science & Technology* 41: 3495–3500.

Salminen, R. (Chief-editor), Batista, M. J., Bidovec, M., Demetriades, A., De Vivo, B., De Vos, W., Duris, M., Gilucis, A., Gregorauskiene, V., Halamic, J., Heitzmann, P., Lima, A., Jordan, G., Klaver, G., Klein, P., Lis, J., Locutura, J., Marsina, K., Mazreku, A., O'Connor, P. J., Olsson, S.Å., Ottesen, R.-T., Petersell, V., Plant, J.A., Reeder, S., Salpeteur, I., Sandström, H., Siewers, U., Steenfelt, A., Tarvainen, T. (2005). *Geochemical Atlas of Europe. Part 1: Background Information, Methodology and Maps*. Espoo, Geological Survey of Finland, 526 pp, 36 fig, 362 maps,

Smolders, E. Oorts, K., Lombi, E., Schoeters, I., Ma, Y., Zrna, S., McLaughlin, M.J. (2012). The Availability of Copper in Soils Historically Amended with Sewage Sludge, Manure and Compost. *Journal of Environmental Quality* 41: 506–514.

Tipping, E. (2005). Modelling Al competition for heavy metal binding by dissolved organic matter in soil and surface waters of acid and neutral pH. *Geoderma* 127: 293–304.

TGD. (1996, revised 2003). EC. 1996/2003. Technical Guidance Document in support of Commission Directive 93/67/EEC on risk assessment for new notified substances, Commission Regulation (EC) No. 1488/94 on risk assessment for existing substances and Directive 98/8/EC of the European Parliament and of the Council concerning the placing of biocidal products on the market, 2003. IHCP/JRC, Ispra, Italy.

Ulén, B. (1995). Episodic precipitation and discharge events and their influence on losses of phosphorus and nitrogen from tile-drained arable fields. *Swedish Journal of Agricultural Sciences* 25: 25–31.

Xue, H. B., Sigg, L., Gachter, R. (2000). Transport of Cu, Zn and Cd in a small agricultural catchment. *Water Research* 34: 2558–2568.

Zhang, X.; Chen, L.; Li, Q.; Qi, X.; Yang, S. (2013). Increase in soil nutrients in intensively managed cash-crop agricultural ecosystems in the Guanting Reservoir Catchment, Beijing, China. *Geoderma* 193–194: 102–108.

Appendices

Appendix 1 Predicted concentrations of copper and zinc in soils, waters and due to soil application of fattening pig manure.

SOILS

Table A1. Predicted total concentrations of copper in topsoil ($\mu\text{g g}^{-1}$; 0-30cm) under 'pristine' conditions and for 2000, 2010, 2020, 2030 and 2060.

Scenario code	Pristine	2000	2010	2020	2030	2060
D1	4.2	10.8	12.0	13.2	14.3	17.6
D2	9.6	20.0	21.4	22.6	23.9	27.6
D3	8.0	15.5	16.9	18.1	19.3	22.9
D4	6.1	11.4	12.6	13.6	14.6	17.6
D5	8.3	13.0	14.1	15.0	16.0	18.8
D6	28.1	33.3	34.5	35.6	36.7	40.0
R1	10.0	16.4	17.7	18.8	19.9	23.1
R2	9.1	12.7	13.3	13.7	14.1	14.9
R3	26.6	33.0	34.0	34.5	35.2	37.1
R4	29.1	30.4	31.1	31.7	32.3	33.7

Table A2. Predicted labile concentrations of copper in topsoil ($\mu\text{g g}^{-1}$; 0-30cm) under 'pristine' conditions and for 2000, 2010, 2020, 2030 and 2060.

Scenario code	Pristine	2000	2010	2020	2030	2060
D1	0.1	3.3	3.8	4.3	4.7	6.0
D2	0.1	5.1	5.7	6.2	6.7	8.1
D3	0.2	5.5	6.4	7.1	7.8	9.9
D4	0.1	3.0	3.5	4.0	4.4	5.8
D5	0.1	2.9	3.5	4.0	4.4	5.8
D6	0.1	2.8	3.3	3.8	4.3	5.6
R1	0.1	3.3	3.8	4.3	4.7	6.0
R2	0.3	3.1	3.4	3.7	3.9	4.4
R3	0.1	4.0	4.3	4.6	4.9	5.6
R4	<0.1	2.2	2.5	2.8	3.1	3.8

Table A3. Predicted total concentrations of zinc in topsoil ($\mu\text{g g}^{-1}$; 0-30cm) under 'pristine' conditions and for 2000, 2010, 2020, 2030 and 2060.

Scenario code	Pristine	2000	2010	2020	2030	2060
D1	18.8	58.8	66.5	73.5	80.4	101
D2	77.7	123	131	138	146	167
D3	30.1	70.7	78.6	85.5	92.4	113
D4	24.2	56.9	63.6	69.7	75.8	93.9
D5	34.0	63.1	69.4	75.2	80.9	97.9
D6	88.2	120	128	135	142	162
R1	53.7	91.9	99.0	105	112	130
R2	70.4	90.9	93.7	95.4	96.9	100
R3	78.6	120	126	131	135	148
R4	114	135	140	144	147	157

Table A4. Predicted labile concentrations of zinc in topsoil ($\mu\text{g g}^{-1}$; 0-30cm) under 'pristine' conditions and for 2000, 2010, 2020, 2030 and 2060.

Scenario code	Pristine	2000	2010	2020	2030	2060
D1	0.3	7.1	7.9	8.8	9.6	11.9
D2	0.3	8.2	9.0	9.9	10.7	13.0
D3	0.1	13.6	15.5	17.2	18.9	23.5
D4	0.2	6.4	7.2	8.0	8.8	11.0
D5	0.3	6.4	7.3	8.2	9.0	11.4
D6	0.2	6.0	6.9	7.7	8.5	10.8
R1	0.3	7.0	7.7	8.5	9.2	11.2
R2	0.1	9.6	10.3	10.7	11.0	11.5
R3	0.2	7.0	7.5	8.0	8.5	9.8
R4	0.1	4.7	5.2	5.6	6.1	7.1

Table A5. Predicted dissolved concentrations of copper in surface water ($\mu\text{g dm}^{-3}$) under 'pristine' conditions and for 2000, 2010, 2020, 2030 and 2060, using an enrichment factor of three.

Scenario code	Pristine	2000	2010	2020	2030	2060
D1 ditch	0.26	2.8	3.2	3.5	3.8	4.6
D1 stream	0.13	0.28	0.31	0.34	0.36	0.42
D2 ditch	0.08	7.1	7.8	8.3	8.8	10.1
D2 stream	0.09	2.3	2.5	2.6	2.8	3.2
D3 ditch	0.12	9.4	10.7	11.7	12.6	15.0
D4 pond	0.36	6.2	7.1	7.8	8.5	10.4
D4 stream	0.09	0.23	0.25	0.27	0.30	0.35
D5 pond	0.26	5.4	6.4	7.1	7.8	9.7
D5 stream	0.09	0.13	0.15	0.16	0.17	0.19
D6 ditch	0.27	1.4	1.7	1.8	2.0	2.5
R1 pond	0.20	0.89	1.0	1.1	1.2	1.5
R1 stream	0.03	0.03	0.03	0.03	0.03	0.03
R2 stream	0.01	0.01	0.01	0.01	0.01	0.01
R3 stream	0.07	0.07	0.07	0.07	0.07	0.08
R4 stream	0.02	0.02	0.03	0.03	0.03	0.03

Table A6. Predicted dissolved concentrations of copper in surface water ($\mu\text{g dm}^{-3}$) under 'pristine' conditions and for 2000, 2010, 2020, 2030 and 2060, not using an enrichment factor.

Scenario code	Pristine	2000	2010	2020	2030	2060
D1 ditch	0.26	2.7	3.1	3.5	3.8	4.5
D1 stream	0.13	0.26	0.29	0.31	0.34	0.39
D2 ditch	0.08	7.0	7.7	8.2	8.7	10.0
D2 stream	0.09	2.1	2.3	2.5	2.7	3.1
D3 ditch	0.12	9.4	10.7	11.7	12.6	15.0
D4 pond	0.36	6.1	7.1	7.8	8.5	10.3
D4 stream	0.09	0.22	0.25	0.27	0.29	0.34
D5 pond	0.26	5.4	6.4	7.1	7.8	9.7
D5 stream	0.09	0.13	0.14	0.15	0.16	0.19
D6 ditch	0.27	1.4	1.7	1.8	2.0	2.5
R1 pond	0.20	0.72	0.84	0.92	1.0	1.2
R1 stream	0.03	0.03	0.03	0.03	0.03	0.03
R2 stream	0.00	0.01	0.01	0.01	0.01	0.01
R3 stream	0.07	0.07	0.07	0.07	0.07	0.07
R4 stream	0.02	0.02	0.02	0.02	0.02	0.03

Table A7. Predicted dissolved concentrations of zinc in surface water ($\mu\text{g dm}^{-3}$) under 'pristine' conditions and for 2000, 2010, 2020, 2030 and 2060, using an enrichment factor of three.

Scenario code	Pristine	2000	2010	2020	2030	2060
D1 ditch	0.42	3.0	3.4	3.8	4.2	5.4
D1 stream	0.21	0.36	0.40	0.43	0.47	0.56
D2 ditch	0.14	6.7	7.7	8.6	9.5	11.9
D2 stream	0.16	3.0	3.4	3.8	4.2	5.3
D3 ditch	0.20	37.6	44.0	49.5	54.7	69.0
D4 pond	0.58	6.1	7.1	8.1	9.0	11.7
D4 stream	0.14	0.25	0.28	0.31	0.34	0.42
D5 pond	0.42	6.1	7.2	8.3	9.3	12.1
D5 stream	0.14	0.19	0.21	0.23	0.24	0.29
D6 ditch	0.43	1.6	1.9	2.1	2.3	3.0
R1 pond	0.33	2.8	3.3	3.7	4.1	5.2
R1 stream	0.05	0.06	0.06	0.06	0.06	0.07
R2 stream	0.01	0.18	0.20	0.22	0.25	0.39
R3 stream	0.12	0.12	0.12	0.12	0.12	0.13
R4 stream	0.04	0.04	0.04	0.04	0.04	0.03

Table A8. Predicted dissolved concentrations of zinc in surface water ($\mu\text{g dm}^{-3}$) under 'pristine' conditions and for 2000, 2010, 2020, 2030 and 2060, not using an enrichment factor.

Scenario code	Pristine	2000	2010	2020	2030	2060
D1 ditch	0.42	2.8	3.3	3.7	4.1	5.2
D1 stream	0.21	0.32	0.35	0.38	0.41	0.49
D2 ditch	0.14	6.4	7.4	8.3	9.1	11.6
D2 stream	0.16	2.6	3.0	3.3	3.7	4.6
D3 ditch	0.20	37.6	44.0	49.5	54.7	69.0
D4 pond	0.58	6.0	7.1	8.1	9.0	11.6
D4 stream	0.14	0.25	0.28	0.30	0.33	0.41
D5 pond	0.42	6.0	7.2	8.2	9.2	12.1
D5 stream	0.14	0.19	0.21	0.22	0.24	0.29
D6 ditch	0.43	1.6	1.9	2.1	2.3	3.0
R1 pond	0.33	2.0	2.3	2.6	2.9	3.7
R1 stream	0.05	0.05	0.05	0.05	0.05	0.05
R2 stream	0.01	0.14	0.17	0.20	0.24	0.43
R3 stream	0.12	0.12	0.12	0.12	0.12	0.12
R4 stream	0.04	0.04	0.03	0.03	0.03	0.03

Table A9. Predicted total concentrations of copper in sediment ($\mu\text{g g}^{-1}$) under 'pristine' conditions and for 2000, 2010, 2020, 2030 and 2060, using an enrichment factor of three.

Scenario code	Pristine	2000	2010	2020	2030	2060
D1 ditch	3.4	44.3	51.6	57.9	63.9	81.0
D1 stream	3.4	44.2	51.5	57.7	63.7	80.8
D2 ditch	4.0	73.1	81.3	88.2	94.9	114
D2 stream	4.0	70.7	78.7	85.4	92.0	111
D3 ditch	8.4	30.2	38.0	46.0	53.9	77.2
D4 pond	4.5	10.1	12.2	14.6	17.2	26.4
D4 stream	5.3	36.7	43.0	48.3	53.5	68.6
D5 pond	8.0	14.4	17.3	20.6	24.2	36.7
D5 stream	9.4	36.3	42.5	47.7	52.8	67.1
D6 ditch	28.1	66.5	75.8	83.6	90.6	110
R1 pond	10.2	49.0	57.4	64.4	70.8	88.5
R1 stream	9.3	49.7	57.0	63.0	68.9	85.3
R2 stream	9.5	31.0	33.4	34.7	35.6	37.1
R3 stream	17.9	70.2	75.0	78.6	82.0	90.8
R4 stream	28.5	52.5	57.0	60.4	63.5	71.4

Table A10. Predicted total concentrations of copper in sediment ($\mu\text{g g}^{-1}$) under 'pristine' conditions and for 2000, 2010, 2020, 2030 and 2060, not using an enrichment factor.

Scenario code	Pristine	2000	2010	2020	2030	2060
D1 ditch	3.0	17.6	20.3	22.7	25.1	32.0
D1 stream	3.0	17.2	19.8	22.2	24.5	31.3
D2 ditch	3.6	31.1	34.5	37.5	40.3	48.7
D2 stream	3.6	28.2	31.4	34.1	36.8	44.7
D3 ditch	8.2	18.8	23.0	27.3	31.4	43.3
D4 pond	4.4	7.0	7.8	8.8	9.8	13.5
D4 stream	5.2	16.2	18.4	20.4	22.4	28.1
D5 pond	7.9	11.8	13.6	15.6	17.8	25.2
D5 stream	9.2	19.0	21.5	23.5	25.5	31.3
D6 ditch	28.0	47.5	51.9	55.6	58.9	67.7
R1 pond	9.9	25.0	28.5	31.5	34.3	42.4
R1 stream	9.0	23.1	25.9	28.3	30.7	37.6
R2 stream	8.7	17.8	19.1	20.0	20.8	22.4
R3 stream	17.7	40.9	43.3	45.3	47.4	53.1
R4 stream	28.4	36.4	38.4	40.1	41.7	46.2

Table A11. Predicted labile concentrations of copper in sediment ($\mu\text{g g}^{-1}$) under 'pristine' conditions and for 2000, 2010, 2020, 2030 and 2060, using an enrichment factor of three and with an acid-volatile sulphide concentration of $0.63 \mu\text{mol g}^{-1}$.

Scenario code	Pristine	2000	2010	2020	2030	2060
D1 ditch	0.15	8.0	9.3	10.5	11.6	14.6
D1 stream	0.13	7.9	9.2	10.4	11.5	14.5
D2 ditch	0.16	13.8	15.4	17.7	20.7	29.3
D2 stream	0.14	12.8	14.2	15.5	17.8	25.9
D3 ditch	0.51	8.3	10.7	13.1	15.4	31.2
D4 pond	0.11	2.1	3.0	3.8	4.7	7.5
D4 stream	0.10	6.6	7.9	9.0	10.0	13.0
D5 pond	0.37	3.8	5.3	7.0	8.7	13.9
D5 stream	0.17	6.7	8.2	9.4	10.5	13.7
D6 ditch	1.08	9.8	11.9	13.6	15.1	23.6
R1 pond	0.52	8.8	10.4	11.7	12.9	16.2
R1 stream	0.14	7.8	9.1	10.2	11.3	14.2
R2 stream	0.31	6.3	6.9	7.3	7.5	7.8
R3 stream	0.09	9.3	10.1	10.7	11.3	12.8
R4 stream	0.04	5.1	5.9	6.5	7.1	8.5

Table A12. Predicted labile concentrations of copper in sediment ($\mu\text{g g}$) under 'pristine' conditions and for 2000, 2010, 2020, 2030 and 2060, not using an enrichment factor and with an acid-volatile sulphide concentration of $0.63 \mu\text{mol g}^{-1}$.

Scenario code	Pristine	2000	2010	2020	2030	2060
D1 ditch	0.08	2.9	3.4	3.8	4.2	5.3
D1 stream	0.05	2.7	3.1	3.5	3.9	5.0
D2 ditch	0.09	5.9	6.5	7.0	7.5	8.9
D2 stream	0.06	4.6	5.2	5.6	6.0	7.2
D3 ditch	0.45	5.2	6.6	8.0	9.4	13.1
D4 pond	0.09	0.93	1.3	1.6	2.0	3.2
D4 stream	0.07	2.3	2.8	3.1	3.5	4.5
D5 pond	0.34	2.7	3.8	4.9	6.1	9.7
D5 stream	0.13	2.8	3.4	3.9	4.3	5.6
D6 ditch	1.07	6.2	7.4	8.3	9.1	11.1
R1 pond	0.47	4.0	4.7	5.3	5.8	7.3
R1 stream	0.09	2.7	3.2	3.6	4.0	5.0
R2 stream	0.11	2.5	2.8	3.1	3.2	3.6
R3 stream	0.04	3.5	3.9	4.2	4.5	5.3
R4 stream	0.02	1.9	2.2	2.5	2.7	3.5

Table A13. Predicted total concentrations of zinc in sediment ($\mu\text{g g}^{-1}$) under 'pristine' conditions and for 2000, 2010, 2020, 2030 and 2060, using an enrichment factor of three.

Scenario code	Pristine	2000	2010	2020	2030	2060
D1 ditch	12.4	264	310	349	387	496
D1 stream	12.4	265	310	349	388	496
D2 ditch	63.2	362	411	452	492	605
D2 stream	63.3	364	413	454	494	607
D3 ditch	28.2	98.6	130	163	197	298
D4 pond	14.7	46.6	59.2	73.5	89.2	144
D4 stream	17.4	210	248	280	312	402
D5 pond	29.6	56.3	67.6	80.5	94.8	145
D5 stream	36.8	193	229	259	288	371
D6 ditch	81.3	259	306	346	384	491
R1 pond	44.7	274	320	359	394	493
R1 stream	44.7	294	337	372	407	503
R2 stream	68.1	181	188	189	189	186
R3 stream	56.3	314	345	369	391	450
R4 stream	124	272	299	320	339	387

Table A14. Predicted total concentrations of zinc in sediment ($\mu\text{g g}^{-1}$) under 'pristine' conditions and for 2000, 2010, 2020, 2030 and 2060, not using an enrichment factor.

Scenario code	Pristine	2000	2010	2020	2030	2060
D1 ditch	8.9	97.6	115	131	146	192
D1 stream	8.8	97.6	115	130	146	192
D2 ditch	59.6	165	184	201	217	267
D2 stream	59.7	166	185	202	218	267
D3 ditch	27.9	44.8	56.1	68.0	80.3	118
D4 pond	13.9	27.3	31.9	37.1	42.9	63.6
D4 stream	16.4	84.4	98.5	111	123	160
D5 pond	28.6	40.0	44.1	49.0	54.3	73.4
D5 stream	35.6	87.9	101	112	123	157
D6 ditch	80.5	144	161	176	191	234
R1 pond	42.2	125	144	160	175	220
R1 stream	42.2	132	149	164	178	222
R2 stream	67.8	115	120	122	124	126
R3 stream	54.0	162	177	191	204	241
R4 stream	122	173	186	196	207	236

Table A15. Predicted labile concentrations of zinc in sediment ($\mu\text{g g}^{-1}$) under 'pristine' conditions and for 2000, 2010, 2020, 2030 and 2060, using an enrichment factor of three and with an acid-volatile sulphide concentration of $0.63 \mu\text{mol g}^{-1}$.

Scenario code	Pristine	2000	2010	2020	2030	2060
D1 ditch	0.36	26.8	35.2	42.4	49.3	68.6
D1 stream	0.34	27.1	35.4	42.6	49.6	69.0
D2 ditch	0.31	42.2	51.0	57.5	62.8	77.4
D2 stream	0.32	41.7	50.5	57.9	64.0	78.9
D3 ditch	0.10	15.0	28.4	42.0	55.6	86.3
D4 pond	0.25	4.2	5.7	7.3	9.0	14.1
D4 stream	0.19	18.4	26.3	32.9	39.4	57.5
D5 pond	0.37	4.4	6.0	7.8	9.5	15.1
D5 stream	0.23	17.6	26.0	33.1	39.9	59.0
D6 ditch	0.36	18.1	28.0	36.4	44.0	60.2
R1 pond	0.44	24.3	33.6	41.1	47.9	66.4
R1 stream	0.28	26.6	34.5	41.1	47.5	64.8
R2 stream	0.07	30.5	33.2	33.6	33.6	31.8
R3 stream	0.22	28.4	33.7	37.9	41.7	51.4
R4 stream	0.13	10.1	14.1	17.9	21.5	30.1

Table A16. Predicted labile concentrations of zinc in sediment ($\mu\text{g g}^{-1}$) under 'pristine' conditions and for 2000, 2010, 2020, 2030 and 2060, not using an enrichment factor and with an acid-volatile sulphide concentration of $0.63 \mu\text{mol g}^{-1}$.

Scenario code	Pristine	2000	2010	2020	2030	2060
D1 ditch	0.16	5.5	6.3	7.1	7.8	9.9
D1 stream	0.13	5.4	6.2	7.0	7.7	9.8
D2 ditch	0.11	6.2	7.1	7.9	8.6	15.9
D2 stream	0.11	6.3	7.2	8.0	8.7	13.8
D3 ditch	0.07	4.1	5.5	6.9	10.1	26.5
D4 pond	0.20	1.7	2.3	2.9	3.6	5.7
D4 stream	0.12	4.6	5.4	6.0	6.7	8.6
D5 pond	0.30	2.0	2.7	3.4	4.2	6.5
D5 stream	0.15	4.4	5.2	5.9	6.6	8.5
D6 ditch	0.31	4.1	5.0	5.8	6.6	13.8
R1 pond	0.30	5.9	6.9	7.7	8.5	12.5
R1 stream	0.12	5.3	6.2	6.9	7.6	9.5
R2 stream	0.02	7.0	7.5	7.7	7.8	7.6
R3 stream	0.09	5.6	6.3	6.9	7.5	9.0
R4 stream	0.05	3.7	4.3	4.8	5.3	6.6

Appendix 2 Changes in predicted topsoil, surface water and sediment metals between IDMM-ag v2 and v3.

Re-evaluation of the IDMM-ag v2 since the draft report submitted November 2015 resulted in some changes to the coding and thus to the model predictions. The changes relevant to risk prediction are summarised in Figure A2.1. All the predictions have changed, but not the overall pattern of variability across the scenario or the surface water types. A single additional incidence of RARs greater than unity is predicted. This is for surface water copper in scenario D5 pond, where the predicted surface water concentrations are approximately double those previously predicted.

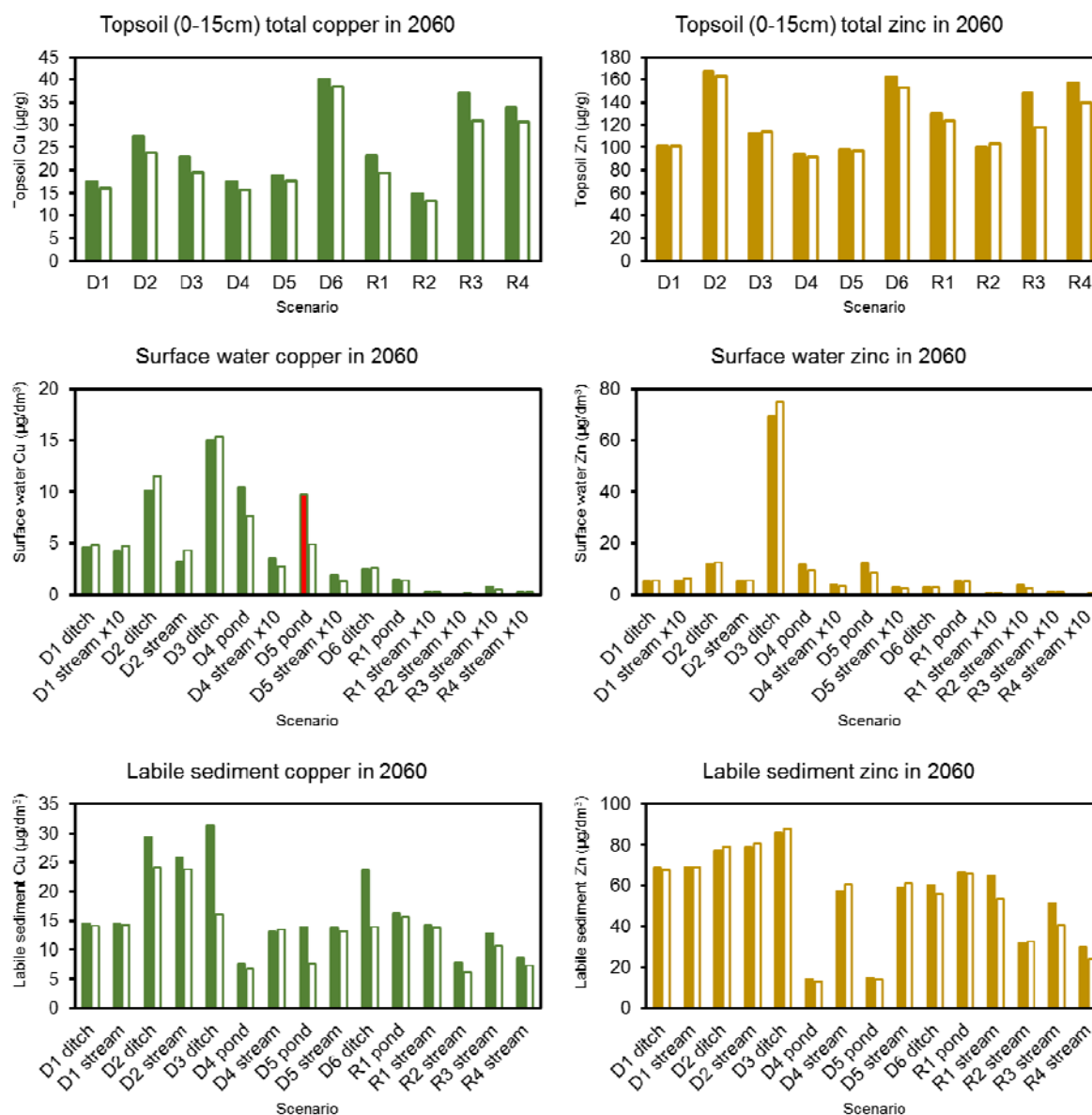


Figure A2.1. Changes in predicted total topsoil metal, dissolved surface water metal and labile sediment metal between IDMM-ag v3 (closed bars) and IDMM-ag v2 (open bars). All concentrations are for the year 2060. Where the IDMM-ag v3 predicts exceedance of the PNEC in 2000 or later where the IDMM-ag v2 does not, the bar is shown in red (this occurs only for dissolved surface water Cu in the D5 pond scenario).



BANGOR
Centre for Ecology & Hydrology
Environment Centre Wales
Deiniol Road
Bangor
Gwynedd
LL57 2UW
United Kingdom
T: +44 (0)1248 374500
F: +44 (0)1248 362133

EDINBURGH
Centre for Ecology & Hydrology
Bush Estate
Penicuik
Midlothian
EH26 0QB
United Kingdom
T: +44 (0)131 4454343
F: +44 (0)131 4453943

LANCASTER
Centre for Ecology & Hydrology
Lancaster Environment Centre
Library Avenue
Bailrigg
Lancaster
LA1 4AP
United Kingdom
T: +44 (0)1524 595800
F: +44 (0)1524 61536

WALLINGFORD - Headquarters
Centre for Ecology & Hydrology
Maclean Building
Benson Lane
Crowmarsh Gifford
Wallingford
Oxfordshire
OX10 8BB
United Kingdom
T: +44 (0)1491 838800
F: +44 (0)1491 692424